iScience

CellPress
OPEN ACCESS

Article

Obesity and metabolic dysfunction drive sex-associated differential disease profiles in hACE2-mice challenged with SARS-CoV-2

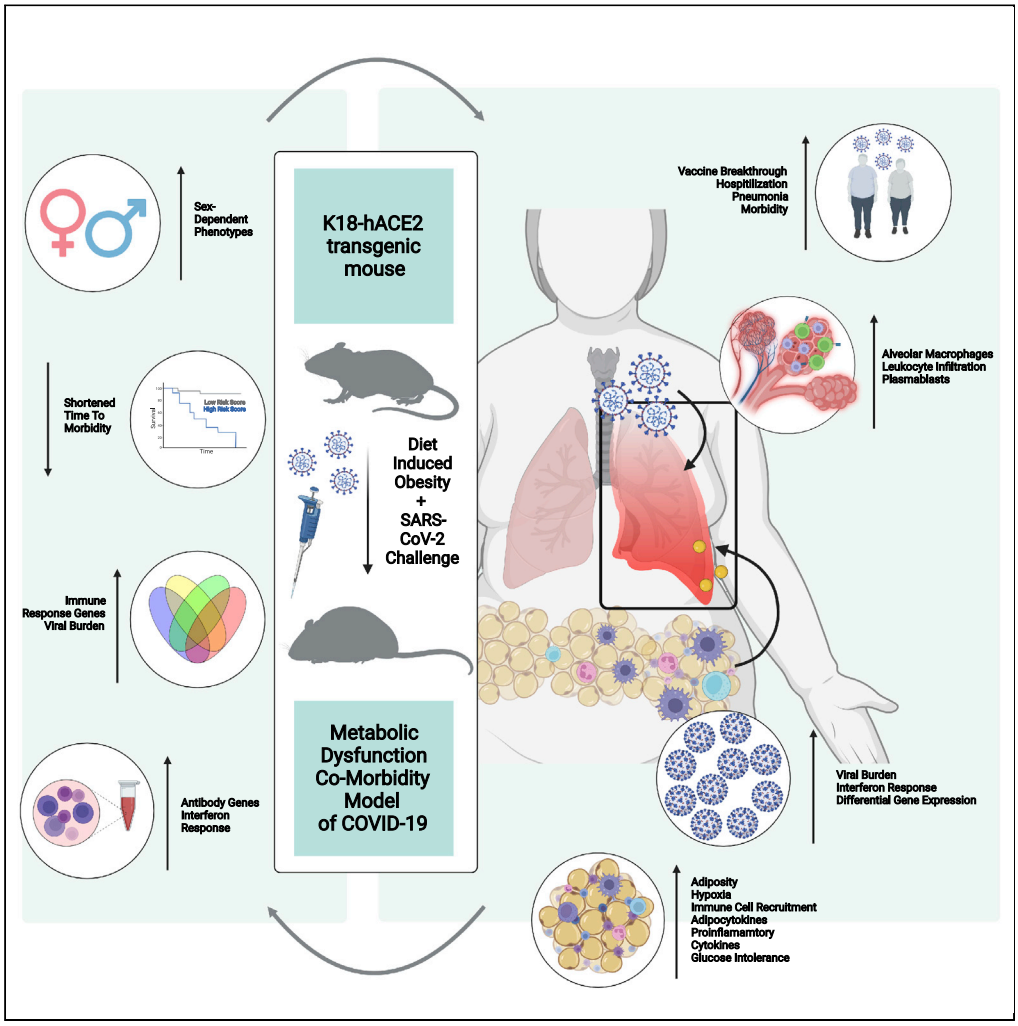

Katherine S. Lee, Brynnan P. Russ, Ting Y. Wong, ..., Ivan Martinez, F. Heath Damron, Holly A. Cyphert

damron40@marshall.edu

Highlights

Transcriptomic analysis of infected lungs revealed unique sex-dependent differences

Obese female mice have high viral RNA burden and interferon production in the lung

Male mice have altered antibody and T cell response gene profiles after viral challenge

Metabolic dysfunction comorbidity can be studied in the hACE2 mouse model of COVID-19

Lee et al., iScience 25, 105038
October 21, 2022
https://doi.org/10.1016/j.isci.2022.105038

iScience

CellPress
OPEN ACCESS

Article

Obesity and metabolic dysfunction drive sex-associated differential disease profiles in hACE2-mice challenged with SARS-CoV-2

Katherine S. Lee,[1,2,5] Brynnan P. Russ,[1,2,5] Ting Y. Wong,[1,2] Alexander M. Horspool,[1,2] Michael T. Winters,[1] Mariette Barbier,[1,2] Justin R. Bevere,[1,2] Ivan Martinez,[1,3] F. Heath Damron,[1,2] and Holly A. Cyphert[4,6,*]

SUMMARY

Severe outcomes from SARS-CoV-2 infection are highly associated with preexisting comorbid conditions like hypertension, diabetes, and obesity. We utilized the diet-induced obesity (DIO) model of metabolic dysfunction in K18-hACE2 transgenic mice to model obesity as a COVID-19 comorbidity. Female DIO, but not male DIO mice challenged with SARS-CoV-2 were observed to have shortened time to morbidity compared to controls. Increased susceptibility to SARS-CoV-2 in female DIO was associated with increased viral RNA burden and interferon production compared to males. Transcriptomic analysis of the lungs from all mouse cohorts revealed sex- and DIO-associated differential gene expression profiles. Male DIO mice after challenge had decreased expression of antibody-related genes compared to controls, suggesting antibody producing cell localization in the lung. Collectively, this study establishes a preclinical comorbidity model of COVID-19 in mice where we observed sex- and diet-specific responses that begin explaining the effects of obesity and metabolic disease on COVID-19 pathology.

INTRODUCTION

Severe acute respiratory syndrome coronavirus 2 (SARS-CoV-2) continues to pose a worldwide epidemiological threat because of the emergence of novel variants with enhanced transmissibility and disease-causing capabilities. Although our understanding of the virus has increased dramatically since its emergence in 2020, questions regarding the mechanisms behind the heterogeneous nature of lethality in human subpopulations remain. Although many infections are asymptomatic or result in mild disease phenotypes, SARS-CoV-2 variants of concern (VOC) remain a considerable threat to at-risk populations where they increase host susceptibility to more severe, deadly infection (Sanyaolu et al., 2020; Djaharuddin et al., 2021; Ng et al., 2021). The most at-risk populations of concern in the COVID-19 pandemic have been suggested to include males, the elderly, pregnant individuals, and those with preexisting conditions such as obesity or metabolic disease which may cause them to be immunocompromised (Centers of Diseases and Control, 2021; Djaharuddin et al., 2021).

It has been shown that more hospitalizations and deaths from COVID-19 have occurred in men than women to-date (Capuano et al., 2020; Nguyen et al., 2021). This matches the widely accepted understanding that the immune response to pathogens is influenced by biological sex. The distribution of genes related to immunological function across the X and Y chromosomes contribute to a generally more robust immune response in females that is dampened in males, and hormonal differences are thought to boost cytokine production in females compared to males (Klein and Flanagan, 2016; Bereshchenko et al., 2018; Takahashi et al., 2020). The exact mechanisms and physiological states which predispose males to morbidity and mortality in COVID-19 are unclear. One early report pointed out that expression of the angiotensin converting enzyme 2 (ACE2) receptor is greater in men than women, which, with hormones and other behavioral tendencies like greater incidence of tobacco and alcohol consumption, may increase susceptibility to virus (Bwire, 2020; Gemmati et al., 2020). Observations that sex-differences exist in diseases contributed to a push in preclinical modeling to incorporate the evaluation of pathophysiology in both sexes, attempting to avoid the potential limitations that just one might provide (Buoncervello et al., 2017; Miller et al., 2017). Although some gaps in knowledge still remain, increased susceptibility to infections in males and

[1]Department of Microbiology, Immunology, and Cell Biology, West Virginia University, Morgantown, WV, USA

[2]Vaccine Development Center at West Virginia University Health Sciences Center, Morgantown, WV, USA

[3]West Virginia University Cancer Institute, School of Medicine, Morgantown, WV, USA

[4]Department of Biological Sciences, Marshall University, Huntington, WV, USA

[5]These authors contributed equally

[6]Lead contact

*Correspondence: damron40@marshall.edu

https://doi.org/10.1016/j.isci.2022.105038

autoimmunity in females have been modeled extensively in preclinical and clinical settings alike (Klein and Flanagan, 2016).

Obesity is another prominent comorbidity in infectious disease that has risen to "epidemic status" in the United States and other countries, occurring at an incidence above 35% in many states (Author Anonymous, 2018; Author Anonymous, n.d.). Obesity is often associated with the subsequent development of comorbidities akin to those which predispose to severe COVID-19 disease outcomes such as type 2 diabetes (T2DM) (Ekoru et al., 2019; Kulcsar et al., 2019; Nowakowska et al., 2019; Bornstein et al., 2020; Pal et al., 2021; Patone et al., 2021). Obesity is often concurrent to metabolic syndrome, a condition marked by "central" obesity with high adiposity, insulin resistance, and high blood glucose (Eckel et al., 2005; Huang, 2009; Paragh et al., 2014). Adiposity (increases in adipose tissue distribution) is accompanied by enlargement of individual adipocytes which become stressed and hypoxic at the cellular level. Chronic exposure to stress signals, hypoxic conditions, and oxidative stress causes adipocytes to produce cytokines like CRP, TNF-alpha, and IL-6 in addition to their healthy secretions intended to maintain homeostasis (Trayhurn, 2013). The resulting recruitment to and activation of proinflammatory-type macrophages cells within the adipose tissue raises basal inflammation systemically in a phenomenon known as "metabolic inflammation" (Gordon, 2003; Ouchi et al., 2011; Park et al., 2014). This inflammation contributes to metabolic dysfunction like insulin resistance in obese persons but also increases susceptibility to pathogens through cellular interactions that are deleterious over time (11-13). COVID-19 also encompasses a complex inflammatory milieu where delayed interferon responses allow virus to continue replicating, meanwhile inciting the proinflammatory actions of neutrophils and lymphocytes that drive the disease-characteristic "cytokine storm" (17). The contributions of preexisting metabolic dysfunction to this aberrant inflammatory response have yet to be mechanistically defined. In laboratory mice, severe outcomes for obese individuals during infection have been modeled for numerous agents including influenza, West Nile virus, and even the parasite *Leishmania* (Smith et al., 2007; Martins et al., 2020; Geerling et al., 2021). Similar studies have implicated preclinical diabetes models as comorbid conditions, but no extensive work has been done to define the comorbid outcomes of SARS-CoV-2 (Zhang et al., 2021).

T2DM is estimated to be the second most common comorbidity in patients with severe COVID-19, resulting in a 2-3 times greater likelihood to succumb compared to healthy persons (Landstra and de Koning, 2021). Over 460 million people worldwide have been diagnosed with diabetes mellitus (either T1DM or T2DM) and greater than 60% of type 2 diabetics are also clinically characterized as obese (Chan et al., 2020). SARS-CoV-2 infection combined with the metabolic dysfunction in T2DM is associated with an increased risk of pneumonia requiring ventilation, ICU admission, and "long COVID" (Unnikrishnan and Misra, 2021). Although COVID-19 vaccine implementation around the world has been a positive effort for protecting vulnerable populations, T2DM has been linked to reduced COVID-19 vaccine efficacy, with lower IgG and neutralizing antibody production (Ali et al., 2021; Pal et al., 2021). Because of their predisposed risk to severe outcomes, defining the immunological profile of patients with T2DM is a necessary step toward solving vaccine-established protection discrepancies.

Most of our knowledge regarding the positive correlation between metabolic dysfunction and SARS-CoV-2 severity comes from retrospective clinical studies, where it becomes impossible to discern the molecular mechanisms that governed severe outcomes (Rawshani et al., 2018, 2021; Barron et al., 2020; Cariou et al., 2020; Chen et al., 2020; Holman et al., 2020; Muniyappa and Gubbi, 2020; Zhu et al., 2020; Demeterco-Berggren et al., 2022). To identify and characterize the mechanisms behind increased infection and severity we developed a preclinical model of disease comorbidities by combining the K18-hACE2 transgenic mouse model and diet-induced obesity (DIO) model where metabolic disease is confirmed by the development of T2DM (Yang et al., 2007; Della Vedova et al., 2016; Avtanski et al., 2019; Bao et al., 2020; Golden et al., 2020; Jiang et al., 2020; Moreau et al., 2020; Muñoz-Fontela et al., 2020; Sun et al., 2020; Winkler et al., 2020; Yinda et al., 2021; Dong et al., 2021). K18-hACE2 mice were subjected to a 60% fat "high-fat," diet for 8 weeks causing measurable obesity, metabolic dysfunction, and hyperglycemia. Normal diet and DIO males and females were either mock challenged or challenged with the Alpha variant of SARS-CoV-2. Female DIO mice were observed to have shorter time to morbidity than normal diet mice and exhibited higher viral RNA burden at the time of terminal euthanasia, indicating sex differences in disease pathology. RNAseq analysis was used to characterize the transcriptional responses of the lung in all experimental cohorts. Systems based analysis revealed DIO mice have unique responses to SARS-CoV-2 challenge including lack of antibody-related gene diversity compared to normal diet K18-hACE2 mice in

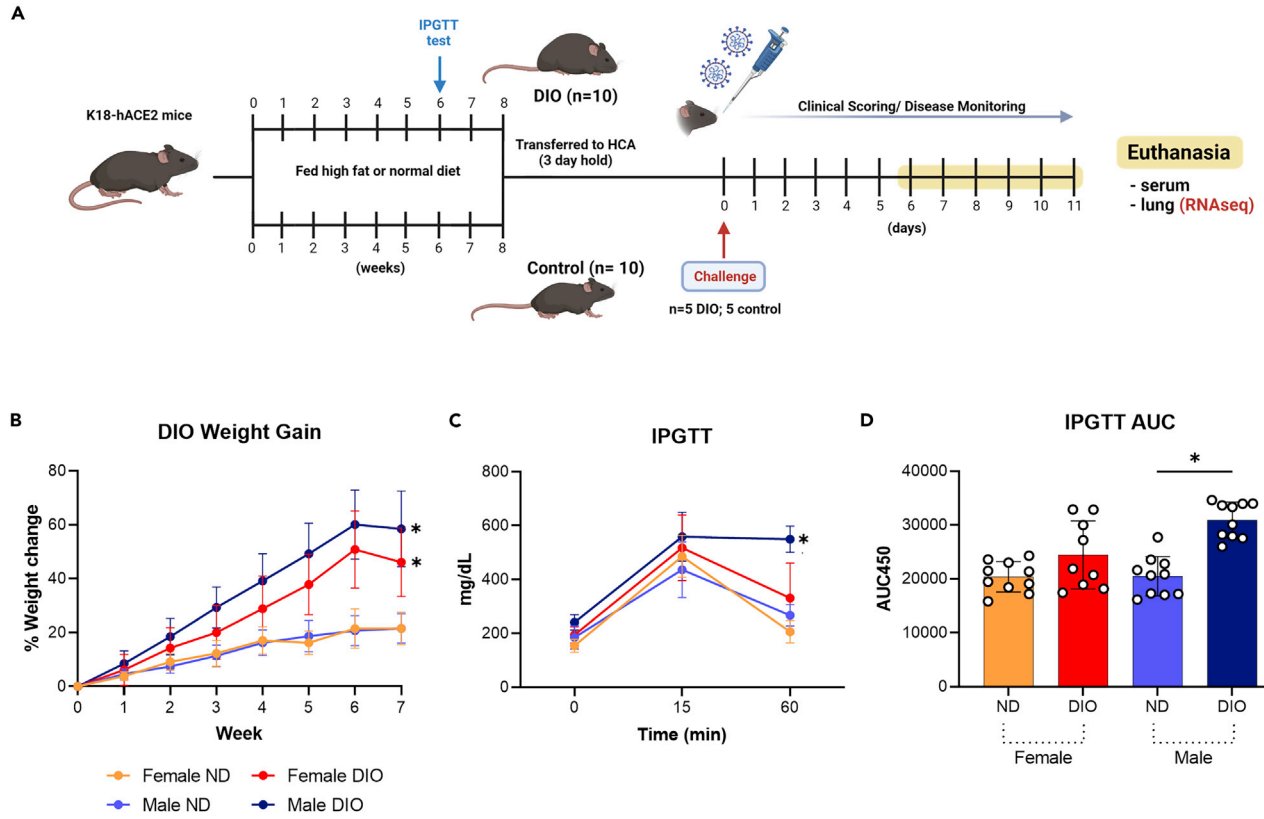

Figure 1. Development of the diet induced obesity (DIO) K18-hACE2 transgenic mouse model

(A) Experimental design: Male and female K18-hACE2 transgenic mice were provided a 60% fat "high fat" diet for 8 weeks to induce glucose impairment consistent with the diet induced obesity (DIO) model then intranasally challenged with 10^3 PFU SARS-CoV-2 Alpha variant. Control groups that were age- and sex-matched remained on normal diet for the entirety of the experiment. (n = 10 diet DIO and 10 normal diet (ND) males; 10 DIO and 10 normal diet females).

(B) Mice in each group were weighed weekly to measure the progression of obesity over 8 weeks (* indicates significance; Multiple unpaired t tests: p=0.000030 female ND versus female DIO; p< 0.000001 male ND versus male DIO); error bars represent SD.

(C and D) Intraperitoneal glucose tolerance testing (IPGTT) was performed at week 6 of the diet intervention to measure glucose clearance and fasting hyperglycemia in male DIO mice ((C) * indicates significance; Multiple unpaired t tests: p< 0.000001 male ND versus male DIO, *P*=ns female ND versus female DIO. (D) One-way ANOVA with Tukey's multiple comparisons test: p< *0.0001* male ND versus male DIO; *P*=ns female ND versus female DIO); error bars represent mean with SD.

addition to differential gene expression profiles. Our data illustrate how metabolic dysfunction can enhance COVID-19 disease and suggest a synergism between hyperglycemia and gene expression profile changes. This data helps to link molecular alterations with infection severity, thus constructing a profile of potential therapeutic targets for the treatment and prevention of death by COVID-19 illness.

RESULTS

K18-hACE2 mice develop obesity, metabolic dysfunction, and hyperglycemia because of high fat diet

The COVID-19 pandemic has illustrated that humans respond to infection with a great deal of heterogeneity. SARS-CoV-2 infection may be lethal in some patients but causes mild or asymptomatic disease in others. Because of this range in infection severity, it is important to understand comorbid conditions to develop therapeutic interventions that support the most at-risk populations. To understand the impact of metabolic dysfunction seen in obesity and type 2 diabetes on the outcomes of viral infection, we utilized a diet-induced model of obesity with K18-hACE2 transgenic mice (Figure 1A). Compared to normal chow mice, DIO mice gained 25% or 37% bodyweight, in females and males respectively (Figure 1B). Intraperitoneal glucose tolerance testing at 6 weeks of an 8-week high-fat or normal diet was utilized to evaluate their ability to clear glucose and therefore assess severity of the DIO phenotype. Glucose tolerance was impaired significantly in male mice receiving the DIO diet (p< 0.000001 male ND versus male DIO) whereas

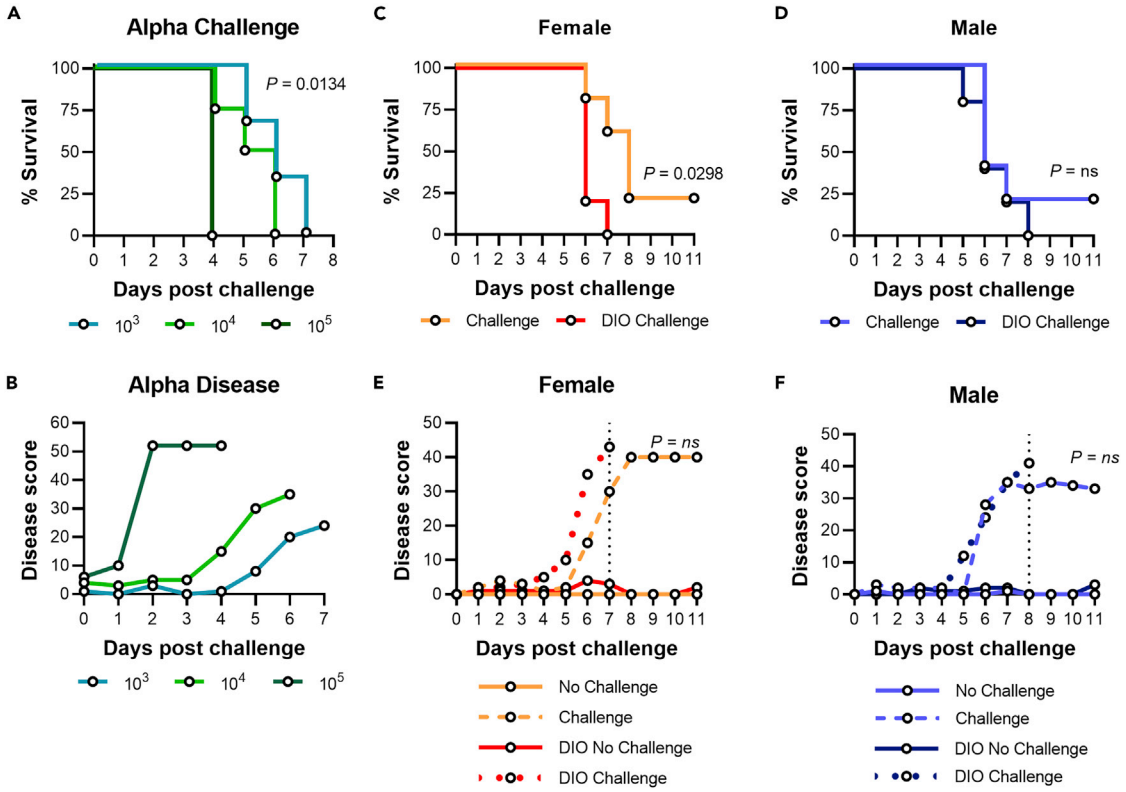

Figure 2. Survival and disease scores of SARS-CoV-2 challenged DIO-K18-hACE2 mice

(A and B) An intranasal challenge dose of 10^3 PFU Alpha SARS-CoV-2 is sufficient for causing disease phenotypes with delayed morbidity in K18-hACE2 mice (10^3 PFU n = 3; 10^4 PFU n = 4; 10^5 PFU n = 5).

(C–F) Survival and cumulative disease scores post-challenge with 10^3 PFU Alpha SARS-CoV-2 were measured for groups of female DIO and normal-diet mice (C and D), as well as male DIO and normal-diet K18-hACE2 mice (E and F). Individual mice euthanized before 11 days post-challenge retain their disease score from the point of morbidity in graphs of cumulative disease scores. Log Rank (Mantel-Cox) tests were utilized to measure the significance level of changes in survival curves. Unpaired t-tests were used to test the significance of disease scores between normal diet and DIO challenge groups. Dotted lines indicate day at which full morbidity of group had been achieved. (n = 10 in panels C, D, E, F) ns = no significance.

female mice presented with non-significant low to mild impairment (Figures 1C and 1D). Despite this observation, DIO females had significantly higher fasting blood glucose levels compared to normal diet females (p=0.0488)(Figure S1). The DIO model has been previously used to study the effects of obesity and type 2 diabetes in mice, and our data here suggest that K18-hACE2-mice on the DIO diet do develop metabolic dysfunction (Della Vedova et al., 2016; Avtanski et al., 2019).

DIO shortens the time to morbidity in lethal SARS-CoV-2 challenge

The Alpha variant (strain B.1.1.7) of SARS-CoV-2 emerged in the UK in the spring of 2021 and moved rapidly across the globe. Alpha was observed to have enhanced virulence compared to ancestral strains of the virus in K18-hACE2-mice and other preclinical animal models (Bayarri-Olmos et al., 2021; Mok et al., 2021; O'Donnell et al., 2021; Radvak et al., 2021; Rosenke et al., 2021; Cochin et al., 2022; T. Y. Wong et al., 2022). Because of the significance of Alpha variant's dominance among circulating strains in humans, we used this VOC to study the effects of DIO and type 2 diabetes in the K18-hACE2 mouse model of SARS-CoV-2 infection. Before the experiment, optimization of viral challenge dose was performed to determine an appropriate dose for achieving symptomatic disease (Figures 2A and 2B). The Alpha strain was intranasally administered to control K18-hACE2 mice at 10^3, 10^4, or 10^5 PFU per dose. Using a previously established disease scoring system (Lee et al., 2022; T. Y. T. Wong et al., 2022b; T. Y. Wong et al., 2022a), we observed that the 10^3 PFU dose caused lethality but postponed the time to morbidity compared to higher doses (Figure 2A) and caused disease phenotypes that increase in severity over time (Figure 2B). DIO and control diet mice were therefore challenged with 10^3 PFU of the Alpha variant to evaluate the effects of comorbidity on SARS-CoV-2 disease outcome. Male and female mice were utilized for DIO challenge studies to account for sex-based predispositions to disease severity (Kadioglu et al., 2011; Klein and Flanagan,

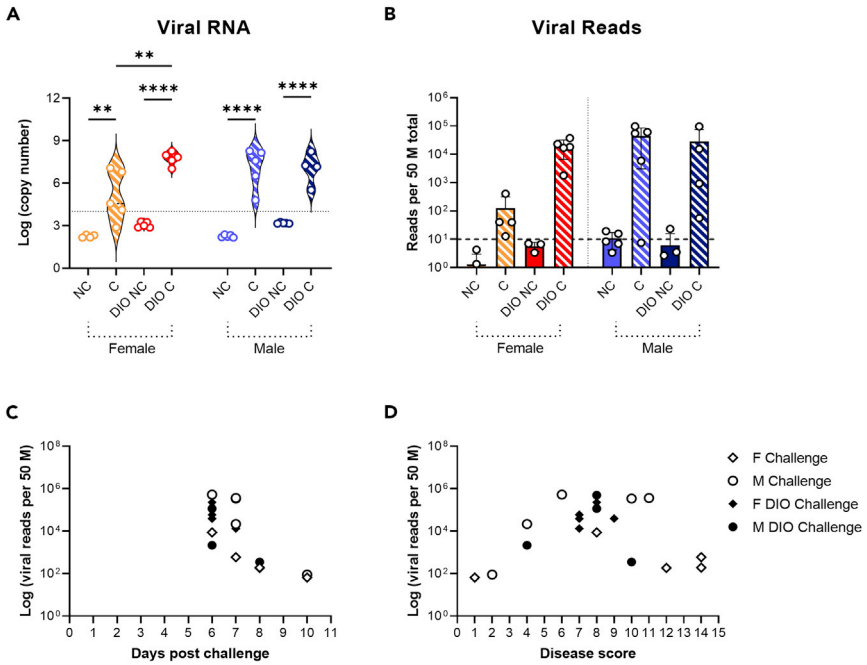

Figure 3. Quantification of viral burden in the lung by qPCR and RNAseq

(A) Viral nucleocapsid RNA was detectable via qPCR in the lung tissue of challenged- and DIO-challenged K18-hACE2 mice (one-way ANOVA**P = 0.0020; ****P=<0.0001). Dotted line indicates limit of detection via qPCR.

(B) SARS-CoV-2 nucleocapsid reads were additionally quantified using RNAseq of lung RNA samples (ns). Dashed line indicates number of RNAseq reads that were examined and determined to be nonspecific. (NC = Normal Diet No Challenge; C=Normal Diet Challenge; DIO NC = DIO No Challenge; DIO C = DIO Challenge); error bars represent mean with SD.

(C and D) To identify correlations between viral RNA burden and disease severity, RNAseq nucleocapsid reads were plotted against host's euthanasia day (C) (Pearson's correlation coefficient: p=0.0308 × versus female challenge, p=0.0161 × versus male challenge, *P*=ns x versus female DIO challenge, *P=ns x* versus *DIO challenge)* and individual disease score at euthanasia (D) (no significant correlations).

2016). DIO shortened the time to morbidity following SARS-CoV-2 challenge in female DIO mice with 0% survival at 7 days after challenge (median time to death = 6 days) compared to only 20% survival in female controls (median time to death = 8 days) (Figure 2C). DIO and normal-diet male mice responded to challenge in a similar manner, with no statistical differences in survival (median time to death = 6 days in both groups). Daily disease scoring over the post-challenge period trended in a similar pattern in DIO and control challenged mice with no sex-dependent differences (Figures 2E and 2F). Collectively, these data suggest that the DIO condition has a greater impact on survival in female mice suggesting that sex specific responses may impact COVID-19 host pathogenesis.

Obese female mice experience greater viral RNA burden in the lungs

To begin identifying the factors that may contribute to the changes in survival that were observed in DIO mice, we next investigated differences in viral burden measured by qRT-PCR analysis of lung tissue for nucleocapsid transcript copy number. Total lung RNA was isolated from mice at euthanasia at their respective humane endpoints. Viral RNA burden was found to be higher in the lungs of DIO female mice than in female normal diet controls and no difference was seen in the viral RNA burden of males (Figure 3A). Normal diet female mice were observed to have approximately 1 million copies of nucleocapsid RNA transcripts on average per lung lobe whereas DIO females have 100-fold more copies, suggesting DIO enhances viral burden in females (Figure 3A). The enhanced viral burden, per PCR analysis, suggested that the differences in time to morbidity and survival in females may be related to viral burden or inability to clear virus.

Transcriptomic analysis of viral RNA confirms females have increased viral RNA due to DIO condition

As a secondary method of evaluating viral burden at morbidity, total lung RNA was used to perform bulk RNAseq analysis to measure the number of virus gene transcripts per total tissue RNA. Viral RNA reads

were mapped to the SARS-CoV-2 reference genome and represented per 50M illumina reads obtained per sample. Total viral reads mirrored the nucleocapsid qRT-PCR analysis (Figure 3B). A 100-fold increase in viral RNA was also observed for DIO females compared to normal females (Figure 3B). To identify correlations between viral burden and morbidity, total viral reads were plotted against the day post-challenge that humane euthanasia occurred (Figure 3C) or against disease score (Figure 3D). High viral reads corresponding to the mortality window 6 days post-challenge were observed for DIO mice where normal diet mice which survived longer underwent euthanasia (because of disease score or planned experimental endpoint) at lower viral burdens. Disease scoring comparisons had greater variance, but DIO mice trended toward having higher viral reads in the lung with higher disease scores (Figure 3D).

Transcriptomic analysis of mouse gene expression profiles unique to metabolic dysfunction

Bulk RNAseq analysis of infected mouse tissues allows for simultaneous pathogen and host transcriptomic analysis (Westermann and Vogel, 2018). We have previously used similar techniques to characterize mouse and bacterial gene expression during infection (Damron et al., 2016; Boehm et al., 2019; Wong et al., 2019). After evaluation of the viral transcriptomics of SARS-CoV-2 challenge in DIO mice, lung tissue RNA from non-challenged, challenged, DIO, or normal diet mice was used to characterize the host transcriptomic responses to SARS-CoV-2. Basic gene expression profiles of biological replicates in the experimental groups were compared using principal component analysis. The transcriptional profiles showed distinct patterns of gene expression between challenge and no challenge groups. Of interest, we observed a higher overlap between DIO and normal-diet in males and female mice than between challenged and non-challenged mice regardless of diet (Figures 4A and 4B). This suggested that challenge with SARS-CoV-2 has a greater impact on the lung transcriptome than diet in K18-hACE2 mice. Separation of the gene profiles into activated and repressed expression bins allowed for visualization of sex-driven differences. DIO induction increased the number of uniquely activated and repressed genes on viral challenge in females but decreased it for males (Figure 4C). Male DIO mice had smaller unique transcriptional profiles (589 DIO male-specific genes) whereas female DIO mice had a much larger transcriptional response (1974 DIO female-specific genes). When the pools of activated genes ($p < 0.05$) from each experimental group were compared using a Venn diagram, the unique gene profiles became narrower, and the unique expression profiles stemming from sex or DIO induction could be appreciated (Figure 4D). Although a core set of 835 genes were found to be activated in all SARS-CoV-2 challenged mice, DIO led to unique transcriptional profiles with differential expression of 765 unique genes in DIO females and 415 unique genes in DIO males. These data suggest that DIO and sex both influence the response to SARS-CoV-2 challenge.

Ingenuity pathway analysis identifies unique canonical pathway matches from metabolic dysfunction and infection

RNAseq analysis showed that the added variables of sex and preexisting comorbidities change the host transcriptional response to SARS-CoV-2 challenge by changing the unique differential gene expression profiles of K18-hACE2 mice. Gene expression fold change data comparing the profiles of each experimental group to no-challenge normal-diet control mice were evaluated by Ingenuity Pathway Analysis (IPA) to identify affected canonical pathways suggested by gene expression. The pathways that were associated with greater positive z-scores in the female DIO challenge datasets implicated activated inflammatory signaling pathways and immune cell activation that were not supported by the expression profiles of DIO no-challenge mice (Figure 5). Male mice's gene expression profiles had altogether similar canonical pathway associations to females. The addition of the DIO condition to challenge groups augmented but did not significantly vary the z-scores of many pathways. Of note, we observed a decreased association of genes within the T cell receptor signaling pathway in male DIO mice. T cell responses are a major contributor to the antiviral response and are heavily implicated in the host response to COVID-19. The magnitude and polyfunctionality of the T cell response in severe cases of COVID-19 is a predictor of outcome as well as the memory response that is protective against reinfection (Peng et al., 2020; Neidleman et al., 2021). Dysregulation of the T cell response early on because of comorbidities may be partially responsible for disease outcome.

We continued our investigation of differential gene expression profiles by narrowing in on specific IPA pathways. To gain preliminary insights into the changes in T cell responses within the different treatment groups, a heatmap of fold changes (compared to sex-matched normal-diet no-challenge groups) in the expression of genes within the T Cell Receptor Signaling pathway was generated. Of interest, male DIO

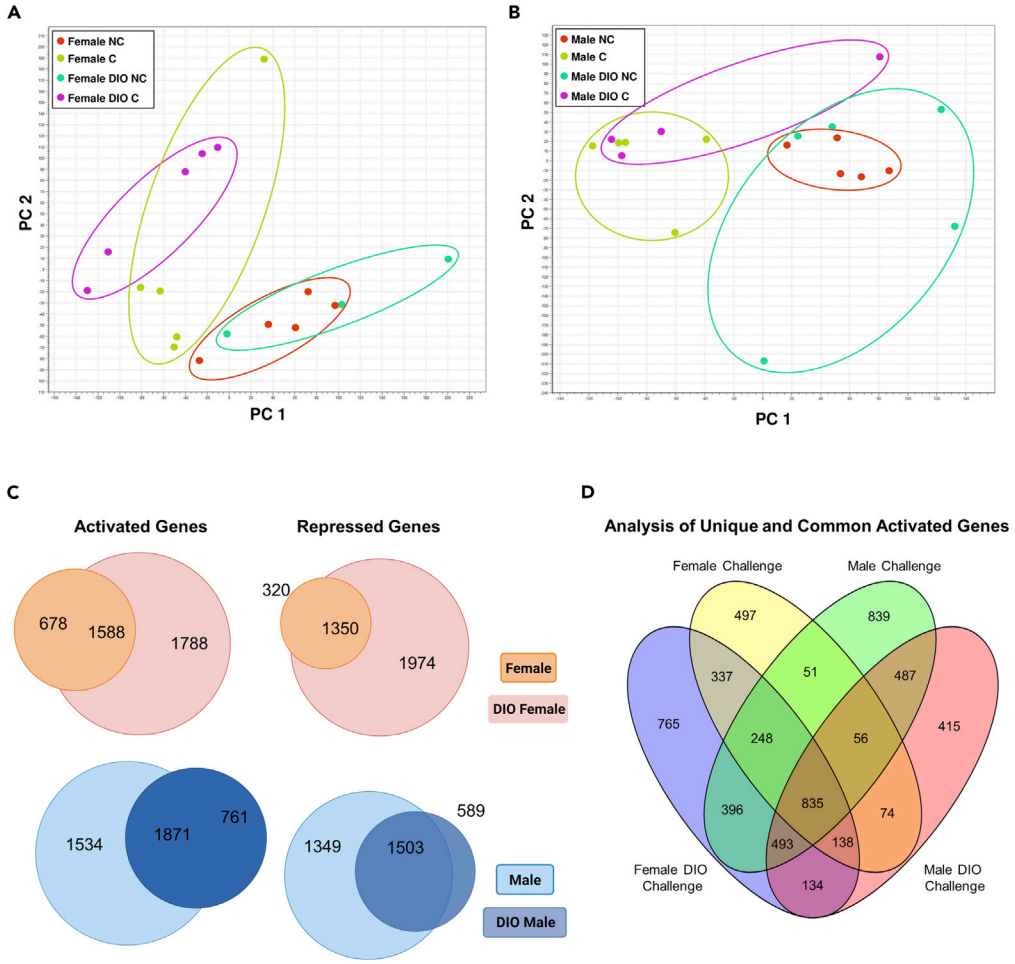

Figure 4. Transcriptomic analysis of lung tissues from Alpha SARS-CoV-2 challenged DIO and normal diet mice

(A and B) Principal component analysis was used to compare differential gene expression profiles of viral challenged DIO or control female (A) and male mice (B).

(C) RNAseq reads from challenged DIO or normal diet mice were compared to no-challenge lean mice to determine relative gene activation or repression. Venn diagrams were used to visualize the unique expression of genes that were specific to experimental condition.

(D) Activated genes from male and female DIO and normal diet mice were compared across experimental conditions to identify unique or conserved genes.

mice had higher expression of numerous T cell-related signaling genes, including many that code for the T cell receptor alpha variable region, without SARS-COV-2 challenge that were low in the male DIO challenge group and both groups of female mice (Figure 6A). Geneslike RelA, which encodes the p65 transcription factor for NF-κB signaling (Ronin et al., 2019), and MAPK13, which encodes the proinflammatory p38 MAP kinase (Salvador et al., 2005) were upregulated in both male and female DIO challenge groups compared to their normal-diet counterparts. However, genes like PDK1 (Sun et al., 2021) and CARD11 (Altin et al., 2011) which support T cell proliferation were high in both normal-diet challenge mice, and comparatively low in both DIO challenge groups. These data suggest DIO resulted in changes in T cell activation. Another pathway of interest was the coronavirus pathway, which is comprised of known biomarkers that are either activated or repressed during SARS-CoV-2 infection (Coronavirus Network Explorer, n.d.). Contrary to the most differential T cell related gene expression occurring in no-challenge DIO males, a large number of inflammatory genes appeared to be up-regulated in challenged DIO females yet repressed in normal-diet females (Figure 6B). NLRP3, encoding for the antiviral inflammasome, was up in DIO females after challenge compared to all other groups, as were genes for the proinflammatory mediators STAT3 and CCL2 (Lai et al., 2017; Chang et al., 2018). It is possible that the gene expression differences that are associated

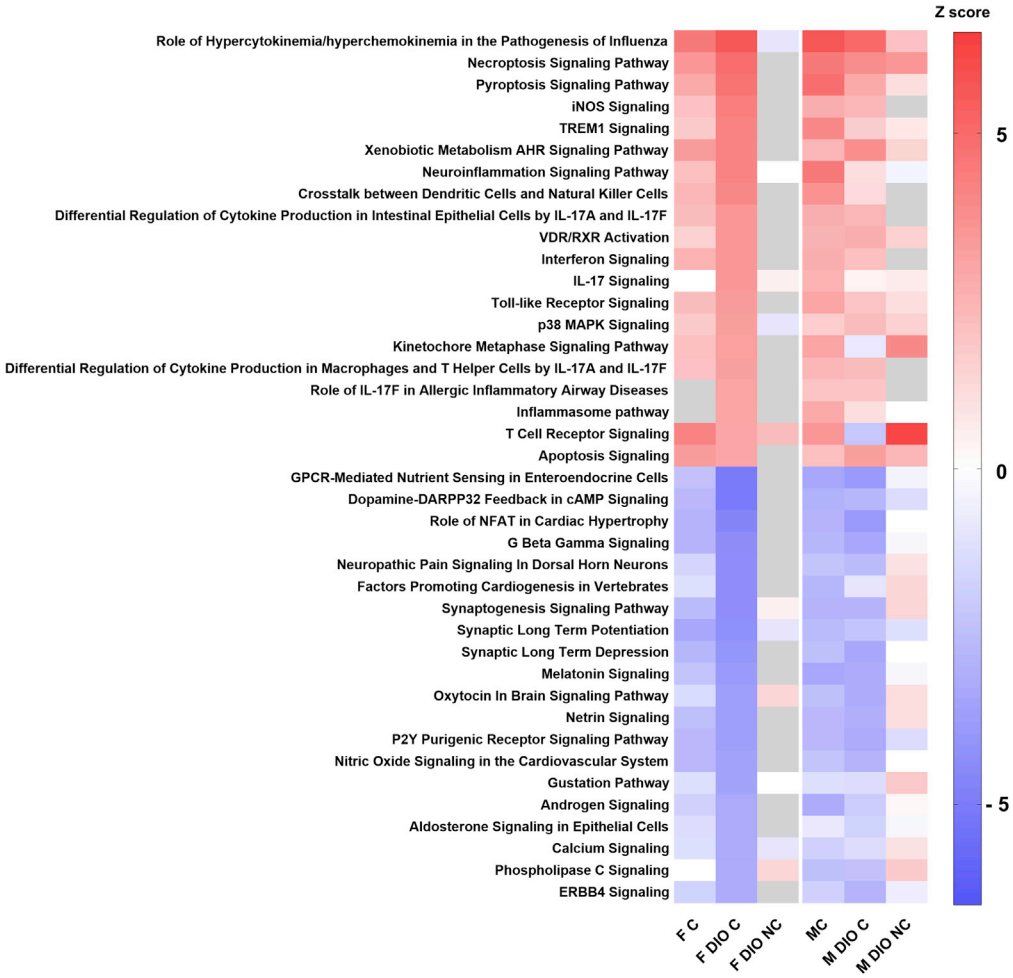

Figure 5. Ingenuity Pathway Analysis of differential gene expression profiles

Fold change values of genes in experimental groups compared to no-challenge were inputted to Ingenuity Pathway Analysis software and sorted into canonical pathways. The highest and lowest 20 canonical pathways by *Z* score in the female DIO challenge group are shown.

with these pathways are directly involved in the impaired viral clearance and affected disease pathogenesis experienced because of the DIO condition.

Metabolic dysfunction in female K18-hACE2 mice heightens host antiviral response profile

To further refine our RNAseq data analysis, Geno Ontology (GO) term analysis was performed to identify biological processes that were affected in our experiment based on the lung tissues' transcriptional profiles. Although DIO induction and sex resulted in different lists of suggested GO terms, a conservative list of terms was present in each analysis that was related to activation of the immune response in viral infection. The terms were graphed with their corresponding enrichment ratio to compare their relevance in the genetic profiles of each experimental condition (Figure 7A). The highest enrichment ratios were seen for the GO terms related to interferon response and were increased in the female DIO challenge sets compared to others. GO terms related to antigen processing and presentation pathways appeared to be absent in both DIO groups. To measure the inflammatory response to virus, the levels of innate cytokines and proinflammatory mediators were measured in serum and lung supernatant collected at euthanasia (Figures S2 and S3). The most striking differences in cytokine production were noted for IFN-γ in the lung (Figure 7B). In females, DIO induction caused an increase in lung supernatant concentrations of IFN-γ compared with normal diet female challenge mice ($p=0.0010$) and DIO male challenge mice ($p=0.0234$) (Figure 7B). No difference was found in the concentrations of

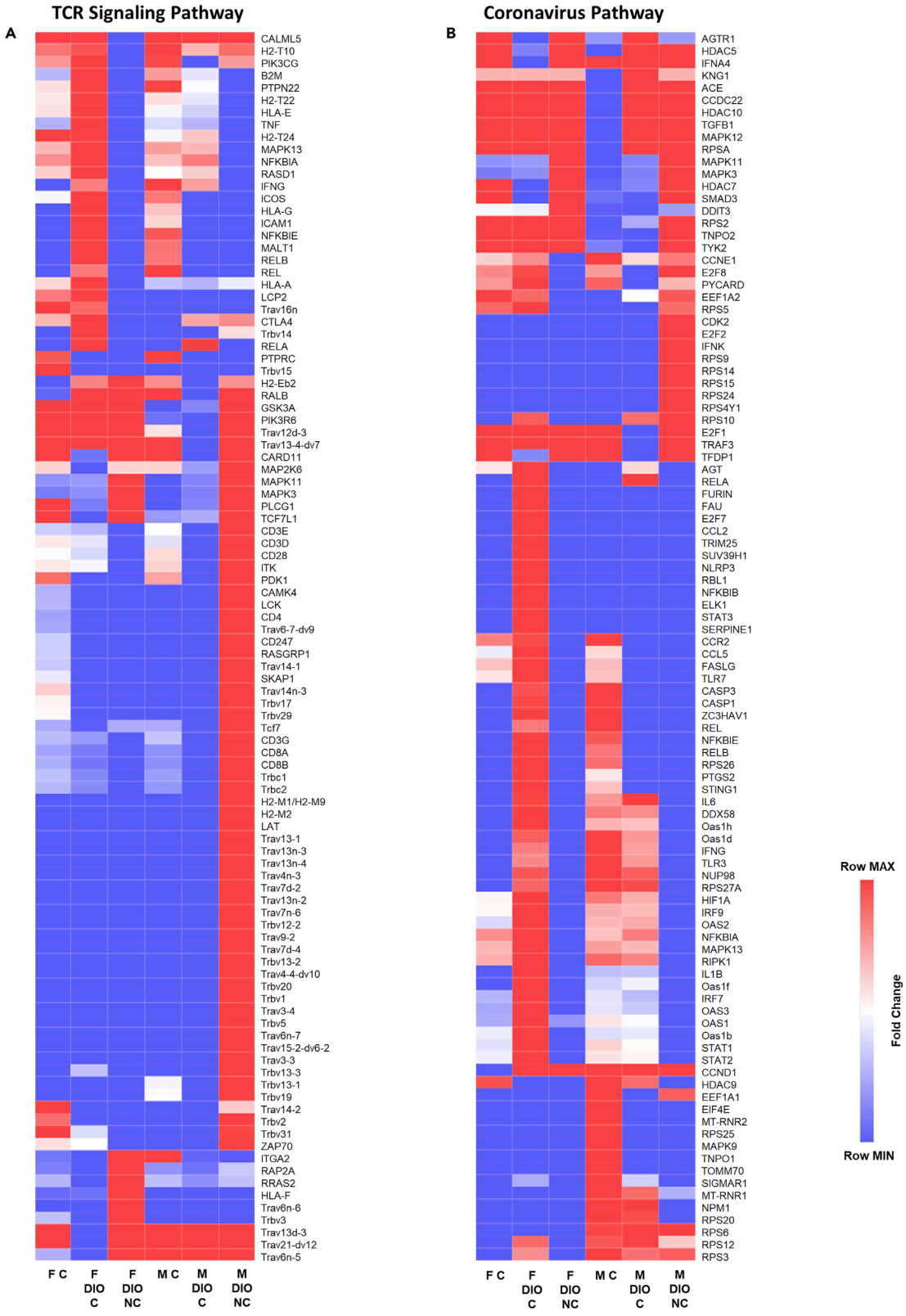
A
TCR Signaling Pathway
CALML5
H2-T10
PIK3CG
B2M
PTPN22
H2-T22
HLA-E
TNF
H2-T24
MAPK13
NFKBIA
RASD1
IFNG
ICOS
HLA-G
ICAM1
NFKBIE
MALT1
RELB
REL
HLA-A
LCP2
Trav16n
CTLA4
Trbv14
RELA
PTPRC
Trbv15
H2-Eb2
RALB
GSK3A
PIK3R6
Trav12d-3
Trav13-4-dv7
CARD11
MAP2K6
MAPK11
MAPK3
PLCG1
TCF7L1
CD3E
CD3D
CD28
ITK
PDK1
CAMK4
LCK
CD4
Trav6-7-dv9
CD247
RASGRP1
Trav14-1
SKAP1
Trav14n-3
Trbv17
Trbv29
Tcf7
CD3G
CD8A
CD8B
Trbc1
Trbc2
H2-M1/H2-M9
H2-M2
LAT
Trav13-1
Trav13n-3
Trav13n-4
Trav4n-3
Trav7d-2
Trav13n-2
Trav7n-6
Trbv12-2
Trav9-2
Trav7d-4
Trbv13-2
Trav4-4-dv10
Trbv20
Trbv1
Trav3-4
Trbv5
Trav6n-7
Trav15-2-dv6-2
Trav3-3
Trbv13-3
Trbv13-1
Trbv19
Trav14-2
Trbv2
Trbv31
ZAP70
ITGA2
RAP2A
RRAS2
HLA-F
Trav6n-6
Trbv3
Trav13d-3
Trav21-dv12
Trav6n-5
F C
F DIO C
F DIO NC
M C
M DIO C
M DIO NC
B
Coronavirus Pathway
AGTR1
HDAC5
IFNA4
KNG1
ACE
CCDC22
HDAC10
TGFB1
MAPK12
RPSA
MAPK11
MAPK3
HDAC7
SMAD3
DDIT3
RPS2
TNPO2
TYK2
CCNE1
E2F8
PYCARD
EEF1A2
RPS5
CDK2
E2F2
IFNK
RPS9
RPS14
RPS15
RPS24
RPS4Y1
RPS10
E2F1
TRAF3
TFDP1
AGT
RELA
FURIN
FAU
E2F7
CCL2
TRIM25
SUV39H1
NLRP3
RBL1
NFKBIB
ELK1
STAT3
SERPINE1
CCR2
CCL5
FASLG
TLR7
CASP3
CASP1
ZC3HAV1
REL
NFKBIE
RELB
RPS26
PTGS2
STING1
IL6
DDX58
Oas1h
Oas1d
IFNG
TLR3
NUP98
RPS27A
HIF1A
IRF9
OAS2
NFKBIA
MAPK13
RIPK1
IL1B
Oas1f
IRF7
OAS3
OAS1
Oas1b
STAT1
STAT2
CCND1
HDAC9
EEF1A1
EIF4E
MT-RNR2
RPS25
MAPK9
TNPO1
TOMM70
SIGMAR1
MT-RNR1
NPM1
RPS20
RPS6
RPS12
RPS3
F C
F DIO C
F DIO NC
M C
M DIO C
M DIO NC
Row MAX
Fold Change
Row MIN

Figure 6. Differential expression of canonical pathways

Heat maps showing the fold change compared to no-challenge of 100 genes in lung RNA from DIO or normal diet mice challenged with SARS-CoV-2 or not within the IPA pathways "T Cell Receptor Signaling" (A) and "Coronavirus Pathogenesis Pathway" (B).

serum IFN-γ across the groups (Figure S3). DIO induction in males did not result in a significant change in IFN-γ production. This is an important finding because IFN-γ production is triggered during SARS-CoV2 infection and is essential for both viral clearance and resolution of the infection (Lee and Ashkar, 2018). Together, these data suggest that changes in the immune response triggered by T2DM/obesity in female mice may hinder positive disease outcomes. As shown above, challenged DIO females had 100-fold higher viral RNA burden in the lung (Figure 3A) and we speculate that the presence of higher levels of viral particles in the lung of DIO females is associated with the increased interferon response observed here.

Sex and metabolic dysfunction influence antibody production

In addition to T cell and interferon response, antibodies also play an important role in the immune response against SARS-CoV-2. RNAseq reads from lung RNA were analyzed to quantify antibody-related gene expression and gain insights into the effects of diet and sex on the humoral response. Overall, a trend was appreciable where antibody genes were highest expressed by male mice challenged with SARS-CoV-2 when reads were mapped and visualized by heatmap (Figure 8A). In male challenged mice, the diversity of upregulated Igh and Igk genes was greater than in the other groups, suggesting: (1) the presence of B cells in the lung, and (2) the unique activation of these B cells in male normal-diet mice after challenge compared to DIO males and both female groups. To determine if changes observed at the mRNA expression level translated into variation in protein antibody responses, quantification of anti-SARS-CoV-2 RBD and anti-nucleocapsid IgG and IgM in serum was performed via ELISA to measure virus-specific antibodies. At this early point after the challenge, only DIO challenged females produced significant levels of anti-RBD IgM antibodies compared to non-challenged female mice. We did not observe statistically significant differences in anti-nucleocapsid IgM, anti-RBD IgG or anti-nucleocapsid IgG between DIO and normal diet groups, likely because of the fact that titers were measured 11 or fewer days post-challenge. Altogether, lung mRNA and circulating serological immunoglobulin data suggest that the humoral response generated by males and females in response to SARS-CoV2 is different, with the female response characterized by higher levels of circulating IgM and the male response characterized by B cell activation and differentiation in the lung.

DISCUSSION

Despite vaccines, antibodies, and small molecule therapeutics, SARS-CoV-2 continues to infect individuals driving continuation of the COVID-19 pandemic. Owing to the heterogeneous nature of COVID-19 cases, it is important to consider the host factors and responses that predispose to severe infection or death. Obesity and type 2 diabetes (T2DM) have long been appreciated as comorbidities for infectious diseases, yet very little controlled experimental data has illuminated how these comorbidities interplay with COVID-19. In addition, sex-specific responses to COVID-19 are obvious in the diversity of disease manifestation (Viveiros et al., 2021). To begin the effort to explore these conditions in preclinical models, we aimed to develop a comorbidity model for COVID-19 based on the previously implicated model of diet induced obesity and T2DM (Figure 1). Utilizing our model, we designed experiments to evaluate sex and DIO as central variables. We utilized the Alpha variant of SARS-CoV-2 which we previously identified as having high virulence compared to ancestral strains (Wong et al., 2022a). K18-hACE2 mice with DIO showed that disease as well as morbidity and mortality were affected very little by the addition of DIO in males; however, the DIO condition greatly affected females (Figure 2) and resulted in 100-fold higher viral RNA burden in the lung (Figure 3). To characterize the augmented host response to viral challenge we utilized RNAseq analysis of the lung tissue to analyze the pathogen-specific airway responses to the presence of virus (Figure 4). Pathway analysis using GO term and Ingenuity Pathway analyses illuminated more sex- and diet-specific responses. Notably, it appeared that DIO non-challenged male mice develop preexisting T cell gene expression signatures in the lungs suggestive of T cell infiltration that is decreased after viral challenge (Figure 6A). DIO seemed to hinder B cell responses in the lungs of challenged male mice (Figures 6, 7, and 8) indicating that although DIO did not affect the development of morbidity in males, it did alter the host response to infection. In female mice, distinctive gene expression profiles were observed between normal diet and DIO mice. Specifically, challenged female mice have low gene expression profiles corresponding to IPA's Coronavirus Pathogenesis Pathway, whereas the

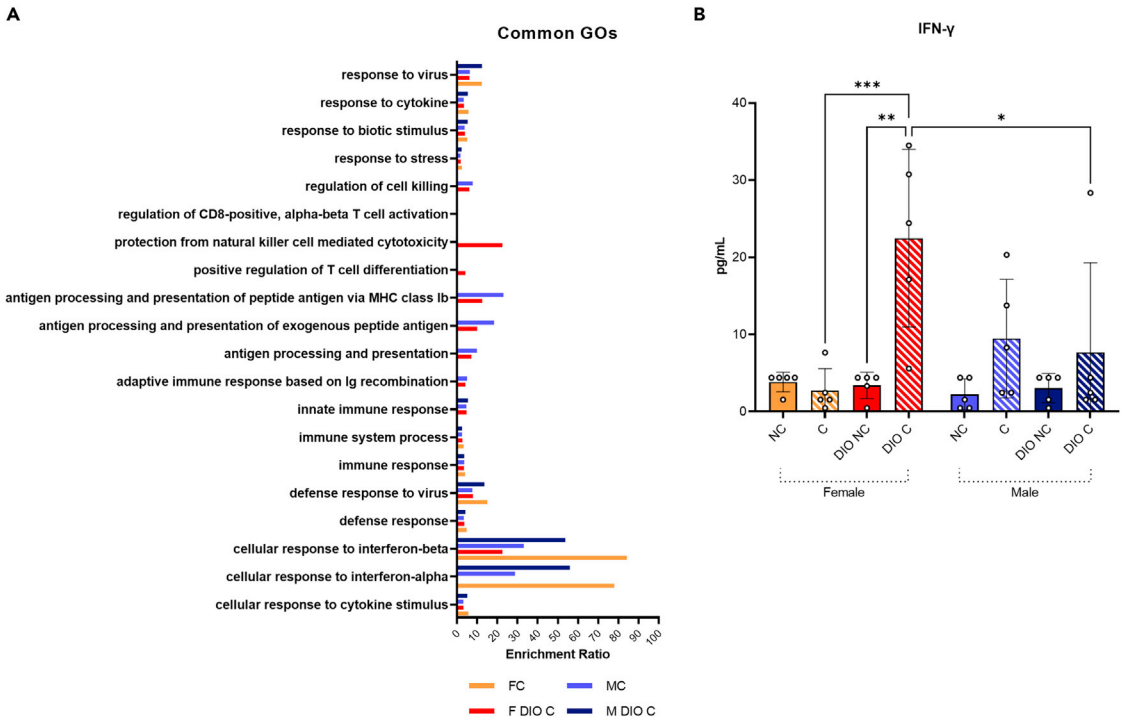

Figure 7. Antiviral response profile of DIO SARS-CoV-2 challenged K18-hACE2 mice

(A) GO terms related to the immune response are graphed to compare term enrichment in experimental groups.

(B) Interferon gamma was measured in the lung supernatant of K18-hACE2 mice at euthanasia. (one-way ANOVA: *P= 0.0234; **P= 0.0015; ***P= 0.0010); error bars represent mean with SD.

addition of the DIO condition enhances many of the pathway's genes (Figure 6). Our data suggest that female K18-hACE2-mice on normal diets have lower viral RNA burden and decreased inflammatory responses, and DIO impairs the clearance of virus in the lung which results in their enhanced morbidity (Figures 2 and 3). The DIO condition appeared to affect female mice more than male mice following SARS-CoV-2 challenge; however, differences were appreciable in males as well. Collectively, these data begin to shed light on the effects of DIO on COVID-19.

To the best of our knowledge this is the first study in K18-hACE2-mice to evaluate DIO and sex utilizing transcriptomic analysis to better understand SARS-CoV-2 VOC-specific host responses. A previous study utilized a mouse-adapted strain of SARS-CoV-2 to challenge DIO C57Bl6 mice to measure the protective efficacy of human convalescent serum treatment (Rathnasinghe et al., 2020, 2021). One correspondence describes a small study where DIO mice were challenged with SARS-CoV-2 and the authors reported increased lung pathology and interferon responses (Zhang et al., 2021). However, the study did not utilize sex comparisons nor did it analyze transcriptomic responses. The high-fat high-carbohydrate diet has been used to evaluate the combined effects of the "Western Diet" and COVID-19 disease in Syrian hamsters (Port et al., 2021). Comparable to what we observed in mice, Western Diet-affected hamsters had increased weight loss, lung pathology, and delayed viral clearance after challenge. Our study does have some caveats that warrant discussion. In our experiment, we only evaluated one SARS-CoV-2 challenge strain, Alpha, and there have now been three VOC strain surges (Beta, Delta, and Omicron) since Alpha was dominantly circulating. In additional studies since then, we have observed enhanced airway inflammation because of challenge with the Delta variant (Lee et al., 2022). We anticipate that different strains would result in variable host responses to what were identified using Alpha; however, additional studies will need to be performed. Another caveat is that only one challenge dose was evaluated (1,000 PFU). If lower or higher challenge doses were to be studied, we would expect to have either shorter or longer time to morbidity during which host response profiles may further develop or remain hidden because of the disease timeline. Finally, our study focused on defining transcriptomic responses to characterize the altered host responses to SARS-CoV-2 challenge. We did not analyze specific cell

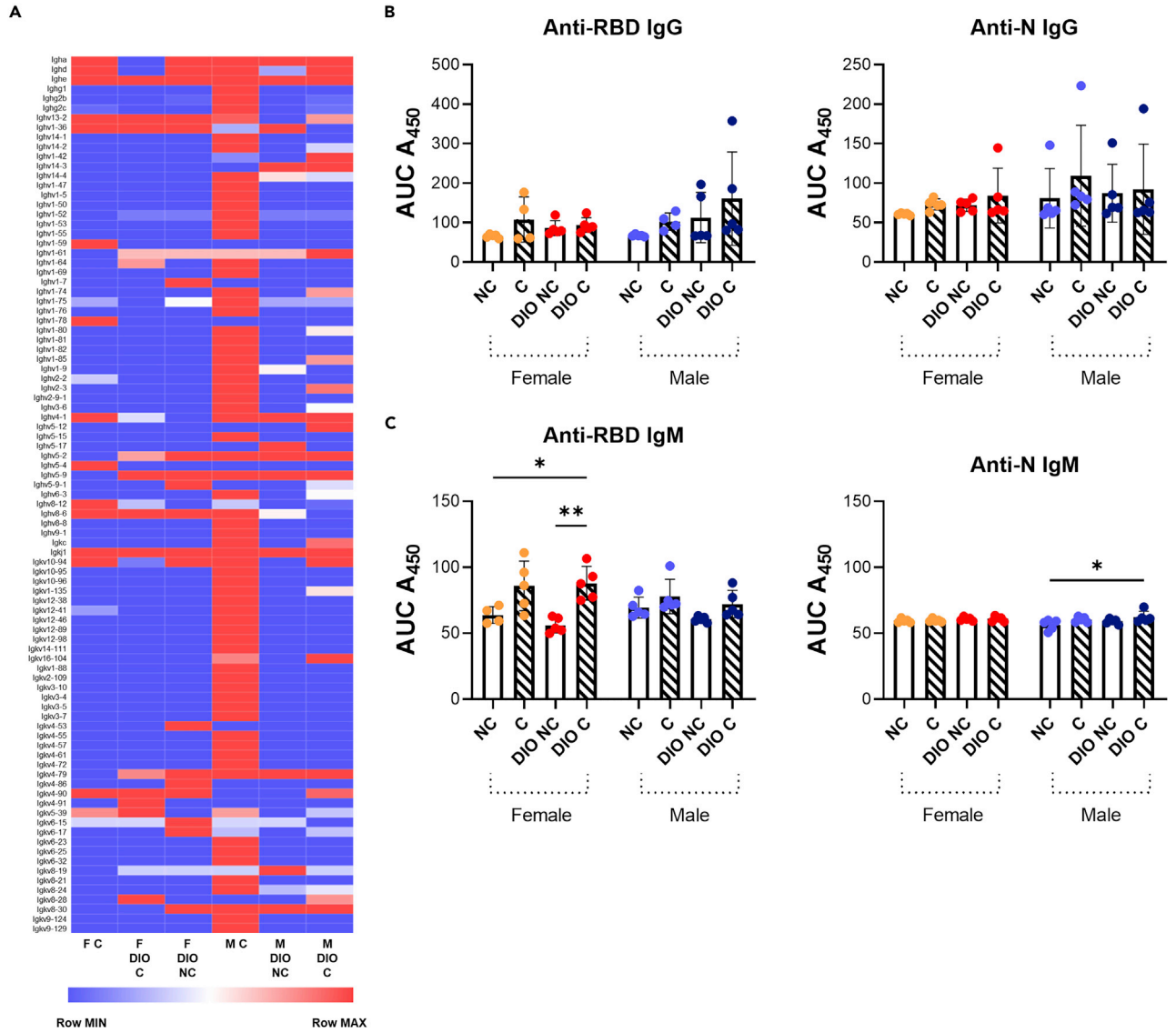

Figure 8. Antibody gene expression because of SARS-CoV-2 in the lungs of DIO K18-hACE2 mice

(A) Antibody gene counts from lung RNA of mice challenged with SARS-CoV-2.

(B and C) Anti-RBD and anti-nucleocapsid (N) IgG and IgM measured in serum of K18-hACE2 mice. (one-way ANOVA: *P< 0.0454; **P = 0.0015); error bars represent mean with SD.

populations through cell isolation and flow cytometry, nor did we evaluate potential mechanisms responsible for this comorbidity.

This model has some limitations for the evaluation of human disease comorbidities and viral pathogenesis. The K18-hACE2 transgenic mouse was generated to act as a lethal model of SARS-COV-2 challenge, and expresses human ACE2 in addition to mouse ACE2 (Moreau et al., 2020; Muñoz-Fontela et al., 2020; Oladunni et al., 2020; R et al., 2020; Winkler et al., 2020; Dong et al., 2021; Yinda et al., 2021). The human ACE2 gene is incorporated into the mouse genome under the human cytokeratin-18 promoter and is thus expressed across tissues and organs in a pattern unlike humans. This leads to greater tissue tropism in the mouse and a propensity for higher viral replication in the brain compared to humans, and detection of viral RNAs in the kidney, spleen, and gastrointestinal tract (Oladunni et al., 2020; Winkler et al., 2020; Kumari et al., 2021; Seehusen et al., 2022). The transgenic incorporation of hACE2 universally also detracts from the model's ability to model comorbid

conditions that may alter ACE2 expression on their own. ACE2 is expressed in adipose tissues, leading to higher ACE2 expression in obesity (Emilsson et al., 2021; Gómez-zorita et al., 2021; Sarver and Wong, 2021). In our 8-week DIO mouse model, hACE2 expression in the lung did not significantly vary between the experimental groups according to RNA sequencing (data not shown). Some additional limitations of the DIO model include a level of sex-based protection from metabolic dysfunction and disease in female mice (Pettersson et al., 2012; Casimiro et al., 2021). At 6 weeks, our study's female DIO K18-hACE2 mice were not as insulin-resistant as males according to IPGTT tests, and some studies suggest that females require a longer period of time on the high fat diet to reach metabolic dysfunction. Despite this, obese female mice in our study achieved hyperglycemia and weight gain as well as displayed worse disease outcomes than obese male mice and female controls, suggesting that some level of comorbid condition had been reached. In future studies by our lab using both female mice and the DIO model, the high fat diet will be utilized for longer periods of time with additional IPGTTs to assess the development of the T2DM-like phenotype.

SARS-CoV-2 infection in humans is generally heterogeneous in symptomology, however, increased susceptibility to severe infection requiring hospitalization are common across patients with T2DM metabolic disease and increased adiposity (obesity) (Ando et al., 2021). The role of elevated glucose and fat accumulation downstream of metabolic dysfunction has been shown in other settings to disturb cellular signaling cascades, promote cytokine synthesis and secretion (leading to hyperinflammation), and increase oxidative stress through enhancement of reactive oxygen species (Giacco and Brownlee, 2010). However, the mechanism by which elevated glucose and adiposity enhance the severity of SAR-CoV-2 infection is still unclear. As demonstrated in our findings, a proinflammatory signature exists basally in T2D hosts and is even further activated in the host response to infection supporting the hypothesis that the preexisting inflammatory state of patients with T2DM and/or obesity is a factor that contributes to the severity of infection and drives an apparent predisposition to negative disease outcomes (Roberts et al., 2021). Our data, with human RNA-Seq analysis from T2DM samples, demonstrates altered immune system activation in response to infection through changes in the antibody response. Human enrichment and GO term analysis in our mouse model compared with lung epithelium from T2DM human patients shows TNF and IL-17 signaling to be highly enriched with several other genes that are involved in the antibody response (Islam et al., 2021). We also saw that T cell populations were augmented across our study groups with male DIO challenged mice demonstrating the most noticeable decrease in T cell subtypes. In severe human COVID-19 cases, it has been demonstrated that a characteristic severe phenotype, lymphocytopenia, is likely associated with $CD4^+$ and $CD8^+$T cell exhaustion (Diao et al., 2020; Mazzoni et al., 2020; Tan et al., 2020; Kusnadi et al., 2021; Rha and Shin, 2021; Xiang et al., 2021). This may be another contributor toward SARS-CoV-2's severity in T2DM. Research surrounding T2DM and obesity pathophysiology has implicated hyperinflammatory macrophages as central agonists in the basal inflammatory state. Melvin et al., using critically ill COVID-19 patient sera, defined the role of macrophages in diabetic COVID-19, showing that coronavirus infection leads to transcription of certain enzymes in the cells that increase their proinflammatory profile including their production of IFN-γ (Melvin et al., 2021). This same phenomenon, while not yet observed in mice, ties into our findings of increased IFN-γ, albeit sex-dependent. Lastly, our RNA-Seq data in normal diet challenge mice compared with normal diet infected patient samples also demonstrates overlap in gene expression profiles relating to a heightened interferon response and cytokine storm which has been previously characterized in humans, highlighting the relevance and use of the K18-hACE2 model (Daamen et al., 2021; Jain et al., 2021). We believe that our model demonstrates some of the pathology that has been seen or suspected in human cohorts including changes in B and T cell signatures and an exaggerated proinflammatory cytokine profile (summarized in Figure 9). Unfortunately, there is still limited data on whole lung tissue samples from diabetic patients to make direct comparisons. Published reports from postmortem lung tissue genomic analysis are often non-separated based on disease presence and patient history is not described (Bass et al., 2021). However, these overlaps in non-comorbid human clinical observations and mouse data are encouraging as modeling SAR-CoV-2 in the laboratory setting is critical for understanding the molecular mechanisms at work.

The T2DM-COVID-19 mouse model has allowed us to observe responses to SARS-CoV-2 challenge augmented by both obesity and sex. It is apparent that DIO affects female mice and enhances viral virulence; however, it is not clear how to best ameliorate this issue using therapeutic interventions. In an earlier study (data unpublished), we evaluated treatment with Baricitinib, a JAK inhibitor that could dampen inflammation caused by SARS-CoV-2. We hypothesized that decreasing inflammation

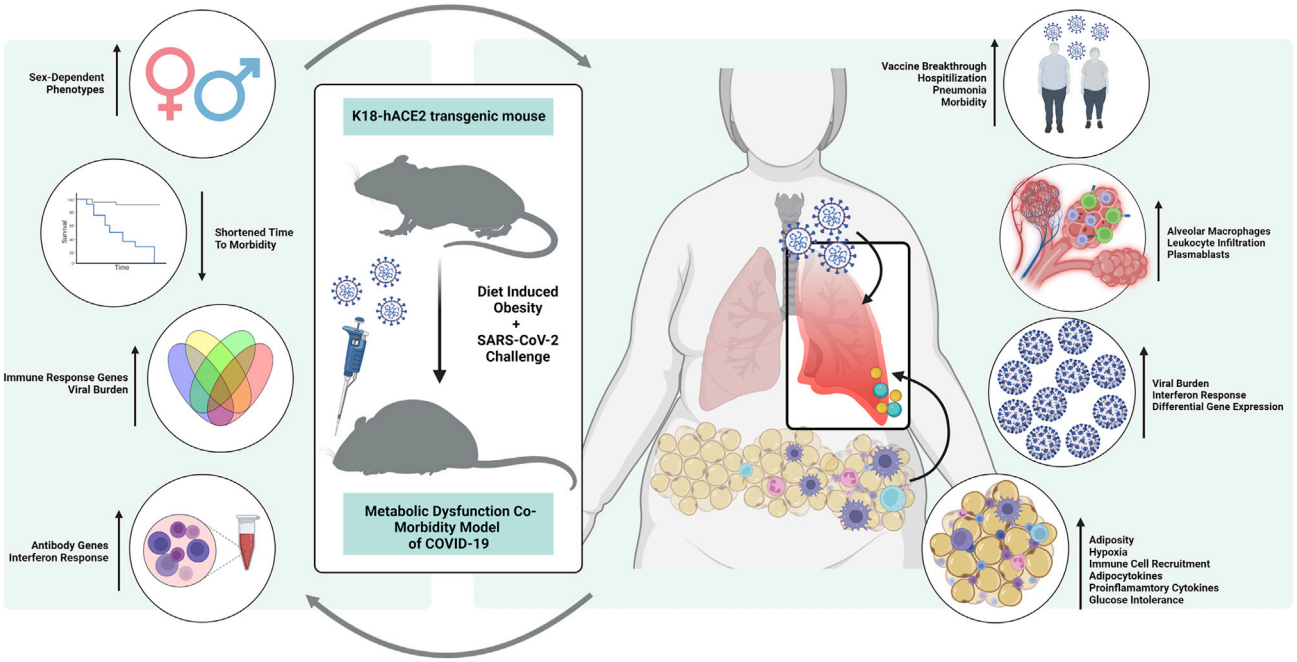

Figure 9. The DIO-COVID-19 mouse model hypothesis: translating mouse data to clinical phenotypes

Our data suggests DIO promotes sex-dependent phenotypes including unique differential gene expression and a shortened time to morbidity when challenged with SARS-CoV-2. Gene expression analysis parallels the changes in viral RNA burden through elevation of immune response genes and the interferon response. As persons with metabolic disease are more likely to succumb to severe SARS-CoV-2 infection and experience vaccine breakthrough, understanding the altered adaptive response is necessary for identifying therapeutic targets. We hypothesize thar hyperglycemia and SARS-CoV-2 infections have a synergistic effect in altering the lung transcriptome in comparison to viral infection alone. Perhaps, it is this synergistic effect that is the central driver of the maladapted immune response.

would improve survival outcomes of SARS-CoV-2-challenged mice; however, the drug did not improve survival of SARS-CoV-2 challenged mice (data not shown). This data leads us to believe that there are still molecular events that underpin overall inflammation as well as a dynamic viral clearance timeline that need to be adjusted to improve protection. Comparing that study with our DIO model, it is clear we need to profile the cell populations that respond to each phase of viral infiltration and identify if they are ineffective at stopping disease progression. Furthermore, we propose that this DIO model can be used to evaluate differences in vaccine-induced immunity among comorbid groups which is rarely evaluated. Future work in our lab will be performed to further define the cellular mechanisms at work in this model with single cell RNA sequencing and timepoint analysis to characterize the evolving host response after challenge. We plan to continue our utilization of the novel DIO-COVID-19 mouse model to uncover therapeutic strategies to improve disease and survival outcomes in diverse persons infected with SARS-CoV-2.

STAR★METHODS

Detailed methods are provided in the online version of this paper and include the following:

- KEY RESOURCES TABLE
- RESOURCE AVAILABILITY
  - Lead contact
  - Materials availability
  - Data and code availability
- EXPERIMENTAL MODEL AND SUBJECT DETAILS
  - Animal ethics statement
  - Biosafety statement
  - High fat diet induced K18-hACE2 mouse model of obesity and type 2 diabetes
  - SARS-CoV-2 challenge strain cultivation
- METHOD DETAILS

SUPPLEMENTAL INFORMATION

Supplemental information can be found online at https://doi.org/10.1016/j.isci.2022.105038.

ACKNOWLEDGMENTS

This project was executed with support from the Vaccine Development Center at the West Virginia University Health Sciences Center. F.H.D. and the VDC are supported by the Research Challenge Grant no. HEPC.dsr.18.6 from the Division of Science and Research, WV Higher Education Policy Commission. We thank BioRender for the use of their software. Lastly, we thank Drs. Laura Gibson and Clay Marsh for supporting this and the lab's additional COVID-19 research efforts.

AUTHOR CONTRIBUTIONS

Studies were designed by F.H.D., H.A.C., K.S.L., B.P.R., J.R.B., and A.M.H. All authors contributed to the execution of the studies. M.T.W. and I.M. prepared and provided titred viral stocks of SARS-CoV-2 for challenge. Animal health checks, necropsy, and tissue processing were performed by F.H.D., T.Y.W., B.P.R., K.S.L., J.R.B., O.A.M., A.M.H., and H.A.C. Viral RNA qPCR was performed by H.A.C. and O.A.M. Serological analysis was executed by K.S.L., B.P.R., and N.A.R. Luminex cytokine assays were completed by BPR. Data was analyzed by K.S.L., B.P.R, H.A.C., and F.H.D. All authors contributed to the writing and revision of this manuscript.

DECLARATION OF INTERESTS

The authors declare no competing interests.

Received: April 26, 2022
Revised: June 25, 2022
Accepted: August 25, 2022
Published: October 21, 2022

REFERENCES

Author Anonymous. (2018). The State of Obesity 2018: Better Policies for a Healthier America. https://www.tfah.org/report-details/state-of-obesity-2021/.

Author Anonymous. Adult Obesity Facts | Overweight & Obesity | CDC. n.d. https://www.cdc.gov/obesity/data/adult.html.

Ali, H., Alterki, A., Sindhu, S., Alahmad, B., Hammad, M., Al-Sabah, S., Alghounaim, M., Jamal, M.H., Aldei, A., Mairza, M.J., et al. (2021). Robust antibody levels in both diabetic and non-diabetic individuals after BNT162b2 mRNA COVID-19 vaccination. Front. Immunol. *12*, 752233. https://doi.org/10.3389/fimmu.2021.752233.

Altin, J.A., Tian, L., Liston, A., Bertram, E.M., Goodnow, C.C., and Cook, M.C. (2011). Decreased T-cell receptor signaling through CARD11 differentially compromises forkhead box protein 3-positive regulatory versus T(H)2 effector cells to cause allergy. J. Allergy Clin. Immunol. *127*, 1277–1285.e5. https://doi.org/10.1016/J.JACI.2010.12.1081.

Ando, W., Horii, T., Uematsu, T., Hanaki, H., Atsuda, K., and Otori, K. (2021). Impact of overlapping risks of type 2 diabetes and obesity on coronavirus disease severity in the United States. Sci. Rep. *11*, 17968. https://doi.org/10.1038/s41598-021-96720-x.

Avtanski, D., Pavlov, V.A., Tracey, K.J., and Poretsky, L. (2019). Characterization of inflammation and insulin resistance in high-fat diet-induced male C57BL/6J mouse model of obesity. Animal Model. Exp. Med. *2*, 252–258. https://doi.org/10.1002/AME2.12084.

Bao, L., Deng, W., Huang, B., Gao, H., Liu, J., Ren, L., Wei, Q., Yu, P., Xu, Y., Qi, F., et al. (2020). The pathogenicity of SARS-CoV-2 in hACE2 transgenic mice. Nature *583*, 830–833. https://doi.org/10.1038/s41586-020-2312-y.

Barron, E., Bakhai, C., Kar, P., Weaver, A., Bradley, D., Ismail, H., Knighton, P., Holman, N., Khunti, K., Sattar, N., et al. (2020). Associations of type 1 and type 2 diabetes with COVID-19-related mortality in England: a whole-population study. Lancet Diabetes Endocrinol. *8*, 813–822.

Bass, A., Liu, Y., and Dakshanamurthy, S. (2021). Single-cell and bulk RNASeq profiling of COVID-19 patients reveal immune and inflammatory mechanisms of infection-induced organ damage. Viruses *13*, 2418. https://doi.org/10.3390/V13122418.

Bayarri-Olmos, R., Johnsen, L.B., Idorn, M., Reinert, L.S., Rosbjerg, A., Vang, S., Hansen, C.B., Helgstrand, C., Bjelke, J.R., Bak-Thomsen, T., et al. (2021). The alpha/b.1.1.7 sars-cov-2 variant exhibits significantly higher affinity for ace-2 and requires lower inoculation doses to cause disease in k18-hace2 mice. Elife *10*, e70002. https://doi.org/10.7554/eLife.70002.

Bereshchenko, O., Bruscoli, S., and Riccardi, C. (2018). Glucocorticoids, sex hormones, and immunity. Front. Immunol. *9*, 1332. https://doi.org/10.3389/FIMMU.2018.01332/BIBTEX.

Boehm, D.T., Varney, M.E., Wong, T.Y., Nowak, E.S., Sen-Kilic, E., Hall, J., Bradford, S.D., DeRoos, K., Bevere, J., Epperly, M., et al. (2019). Characterizing the innate and adaptive responses of immunized mice to Bordetella pertussis infection using in vivo imaging and transcriptomic analysis. Preprint at bioRxiv. https://doi.org/10.1101/674408.

Bornstein, S.R., Dalan, R., Hopkins, D., Mingrone, G., and Boehm, B.O. (2020). Endocrine and metabolic link to coronavirus infection. Nat. Rev. Endocrinol. *16*, 297–298. https://doi.org/10.1038/s41574-020-0353-9.

Buoncervello, M., Marconi, M., Carè, A., Piscopo, P., Malorni, W., and Matarrese, P. (2017). Preclinical models in the study of sex differences. Clin. Sci. *131*, 449–469. https://doi.org/10.1042/CS20160847.

Bwire, G.M. (2020). Coronavirus: why men are more vulnerable to covid-19 than women? SN Compr. Clin. Med. *2*, 874–876. https://doi.org/10.1007/S42399-020-00341-W.

Capuano, A., Rossi, F., and Paolisso, G. (2020). Covid-19 kills more men than women: an overview of possible reasons. Front. Cardiovasc. Med. *7*, 131. https://doi.org/10.3389/FCVM.2020.00131/BIBTEX.

Cariou, B., Hadjadj, S., Wargny, M., Pichelin, M., Al-Salameh, A., Allix, I., Amadou, C., Arnault, G., Baudoux, F., Bauduceau, B., et al. (2020). Phenotypic characteristics and prognosis of inpatients with COVID-19 and diabetes: the CORONADO study. Diabetologia *63*, 1500–1515.

Casimiro, I., Stull, N.D., Tersey, S.A., and Mirmira, R.G. (2021). Phenotypic sexual dimorphism in response to dietary fat manipulation in C57BL/6J mice. J. Diabet. Complicat. *35*, 107795. https://doi.org/10.1016/J.JDIACOMP.2020.107795.

Centers of Diseases and Control (2021). People with Certain Medical Conditions (Centers for Disease Control and Prevention), pp. 1–6. https://www.cdc.gov/coronavirus/2019-ncov/need-extra-precautions/people-with-medical-conditions.html.

Chan, J.C.N., Lim, L.L., Wareham, N.J., Shaw, J.E., Orchard, T.J., Zhang, P., Lau, E.S.H., Eliasson, B., Kong, A.P.S., Ezzati, M., et al. (2020). The Lancet Commission on diabetes: using data to transform diabetes care and patient lives. Lancet *396*, 2019–2082. https://doi.org/10.1016/S0140-6736(20)32374-6.

Chang, Z., Wang, Y., Zhou, X., and Long, J.E. (2018). STAT3 roles in viral infection: antiviral or proviral? Future Virol. *13*, 557–574. https://doi.org/10.2217/FVL-2018-0033.

Chen, Y., Yang, D., Cheng, B., Chen, J., Peng, A., Yang, C., Liu, C., Xiong, M., Deng, A., Zhang, Y., et al. (2020). Clinical characteristics and outcomes of patients with diabetes and COVID-19 in association with glucose-lowering medication. Diabetes Care *43*, 1399–1407.

Cochin, M., Luciani, L., Touret, F., Driouich, J.S., Petit, P.R., Moureau, G., Baronti, C., Laprie, C., Thirion, L., Maes, P., et al. (2022). The SARS-CoV-2 Alpha variant exhibits comparable fitness to the D614G strain in a Syrian hamster model. Commun. Biol. *5*, 225. https://doi.org/10.1038/s42003-022-03171-9.

Coronavirus Network Explorer, n.d. https://digitalinsights.qiagen.com/coronavirus-network-explorer/.

Daamen, A.R., Bachali, P., Owen, K.A., Kingsmore, K.M., Hubbard, E.L., Labonte, A.C., Robl, R., Shrotri, S., Grammer, A.C., and Lipsky, P.E. (2021). Comprehensive transcriptomic analysis of COVID-19 blood, lung, and airway. Sci. Rep. *11*, 7052. https://doi.org/10.1038/s41598-021-86002-x.

Damron, F.H., Oglesby-Sherrouse, A.G., Wilks, A., and Barbier, M. (2016). Dual-seq transcriptomics reveals the battle for iron during Pseudomonas aeruginosa acute murine pneumonia. Sci. Rep. *6*, 39172. https://doi.org/10.1038/srep39172.

Demeterco-Berggren, C., Ebekozien, O., Rompicherla, S., Jacobsen, L., Accacha, S., Gallagher, M.P., Todd Alonso, G., Seyoum, B., Vendrame, F., Haw, J.S., et al. (2022). Age and hospitalization risk in people with type 1 diabetes and COVID-19: data from the T1D exchange surveillance study. J. Clin. Endocrinol. Metab. *107*, 410–418. https://doi.org/10.1210/CLINEM/DGAB668.

Diao, B., Wang, C., Tan, Y., Chen, X., Liu, Y., Ning, L., Chen, L., Li, M., Liu, Y., Wang, G., et al. (2020). Reduction and functional exhaustion of T cells in patients with coronavirus disease 2019 (COVID-19). Front. Immunol. *11*, 827. https://doi.org/10.3389/fimmu.2020.00827.

Djaharuddin, I., Munawwarah, S., Nurulita, A., Ilyas, M., Tabri, N.A., and Lihawa, N. (2021). Comorbidities and mortality in COVID-19 patients. Gac. Sanit. *35* (*Suppl 2*), S530–S532. https://doi.org/10.1016/J.GACETA.2021.10.085.

Dong, W., Mead, H., Tian, L., Park, J.G., Garcia, J.I., Jaramillo, S., Barr, T., Kollath, D.S., Coyne, V.K., Stone, N.E., et al. (2021). The K18-hACE2 transgenic mouse model recapitulates non-severe and severe COVID-1 19 in response to infectious dose of SARS-CoV-2 virus. J. Virol. *96*, e0096421. https://doi.org/10.1128/JVI.00964-21.

Eckel, R.H., Grundy, S.M., and Zimmet, P.Z. (2005). The metabolic syndrome. Lancet *365*, 1415–1428. https://doi.org/10.1016/S0140-6736(05)66378-7.

Ekoru, K., Doumatey, A., Bentley, A.R., Chen, G., Zhou, J., Shriner, D., Fasanmade, O., Okafor, G., Eghan, B., Jr., Agyenim-Boateng, K., et al. (2019). Type 2 diabetes complications and comorbidity in Sub-Saharan Africans. EClinicalMedicine *16*, 30–41. https://doi.org/10.1016/j.eclinm.2019.09.001.

Emilsson, V., Gudmundsson, E.F., Aspelund, T., Jonsson, B.G., Gudjonsson, A., Launer, L.J., Lamb, J.R., Gudmundsdottir, V., Jennings, L.L., and Gudnason, V. (2021). Serum levels of ACE2 are higher in patients with obesity and diabetes. Obes. Sci. Pract. *7*, 239–243. https://doi.org/10.1002/OSP4.472.

Geerling, E., Stone, E.T., Steffen, T.L., Hassert, M., Brien, J.D., and Pinto, A.K. (2021). Obesity enhances disease severity in female mice following West Nile virus infection. Front. Immunol. *12*, 739025. https://doi.org/10.3389/fimmu.2021.739025.

Gemmati, D., Bramanti, B., Serino, M.L., Secchiero, P., Zauli, G., and Tisato, V. (2020). COVID-19 and individual genetic susceptibility/receptivity: role of ACE1/ACE2 genes, immunity, inflammation and coagulation. Might the double X-chromosome in females Be protective against SARS-CoV-2 compared to the single X-chromosome in males? Int. J. Mol. Sci. *21*, E3474. https://doi.org/10.3390/IJMS21103474.

Giacco, F., and Brownlee, M. (2010). Oxidative stress and diabetic complications. Circ. Res. *107*, 1058–1070. https://doi.org/10.1161/CIRCRESAHA.110.223545.

Golden, J.W., Cline, C.R., Zeng, X., Garrison, A.R., Carey, B.D., Mucker, E.M., White, L.E., Shamblin, J.D., Brocato, R.L., Liu, J., et al. (2020). Human angiotensin-converting enzyme 2 transgenic mice infected with SARS-CoV-2 develop severe and fatal respiratory disease. JCI Insight *5*, 142032. https://doi.org/10.1172/JCI.INSIGHT.142032.

Gómez-Zorita, S., Milton-Laskibar, I., García-Arellano, L., González, M., and Portillo, M.P. (2021). An overview of adipose tissue ACE2 modulation by diet and obesity. Potential implications in COVID-19 infection and severity. Int. J. Mol. Sci. *22*, 7975. https://doi.org/10.3390/IJMS22157975.

Gordon, S. (2003). Alternative activation of macrophages. Nat. Rev. Immunol. *3*, 23–35. https://doi.org/10.1038/nri978.

Holman, N., Knighton, P., Kar, P., O'Keefe, J., Curley, M., Weaver, A., Barron, E., Bakhai, C., Khunti, K., Wareham, N.J., et al. (2020). Risk factors for COVID-19-related mortality in people with type 1 and type 2 diabetes in England: a population-based cohort study. Lancet Diabetes Endocrinol. *8*, 823–833.

Horspool, A.M., Kieffer, T., Russ, B.P., DeJong, M.A., Wolf, M.A., Karakiozis, J.M., Hickey, B.J., Fagone, P., Tacker, D.H., Bevere, J.R., et al. (2021). Interplay of antibody and cytokine production reveals CXCL13 as a potential novel biomarker of lethal SARS-CoV-2 infection. mSphere *6*. https://doi.org/10.1128/MSPHERE.01324-20.

Huang, P.L. (2009). A comprehensive definition for metabolic syndrome. Dis. Model. Mech. *2*, 231–237. https://doi.org/10.1242/DMM.001180.

Hulsen, T., de Vlieg, J., and Alkema, W. (2008). BioVenn - a web application for the comparison and visualization of biological lists using area-proportional Venn diagrams. BMC

Genom. *9*, 488. https://doi.org/10.1186/1471-2164-9-488.

Islam, M.B., Chowdhury, U.N., Nain, Z., Uddin, S., Ahmed, M.B., and Moni, M.A. (2021). Identifying molecular insight of synergistic complexities for SARS-CoV-2 infection with pre-existing type 2 diabetes. Comput. Biol. Med. *136*, 104668–104825. https://doi.org/10.1016/j.compbiomed.2021.104668.

Jain, R., Ramaswamy, S., Harilal, D., Uddin, M., Loney, T., Nowotny, N., Alsuwaidi, H., Varghese, R., Deesi, Z., Alkhajeh, A., et al. (2021). Host transcriptomic profiling of COVID-19 patients with mild, moderate, and severe clinical outcomes. Comput. Struct. Biotechnol. J. *19*, 153–160. https://doi.org/10.1016/J.CSBJ.2020.12.016.

Jiang, R.D., Liu, M.Q., Chen, Y., Shan, C., Zhou, Y.W., Shen, X.R., Li, Q., Zhang, L., Zhu, Y., Si, H.R., et al. (2020). Pathogenesis of SARS-CoV-2 in transgenic mice expressing human angiotensin-converting enzyme 2. Cell *182*, 50–58.e8. https://doi.org/10.1016/J.CELL.2020.05.027.

Kadioglu, A., Cuppone, A.M., Trappetti, C., List, T., Spreafico, A., Pozzi, G., Andrew, P.W., and Oggioni, M.R. (2011). Sex-based differences in susceptibility to respiratory and systemic pneumococcal disease in mice. J. Infect. Dis. *204*, 1971–1979. https://doi.org/10.1093/INFDIS/JIR657.

Klein, S.L., and Flanagan, K.L. (2016). Sex differences in immune responses. Nat. Rev. Immunol. *16*, 626–638. https://doi.org/10.1038/nri.2016.90.

Kulcsar, K.A., Coleman, C.M., Beck, S.E., and Frieman, M.B. (2019). Comorbid diabetes results in immune dysregulation and enhanced disease severity following MERS-CoV infection. JCI Insight *4*, 131774. https://doi.org/10.1172/JCI.INSIGHT.131774.

Kumari, P., Rothan, H.A., Natekar, J.P., Stone, S., Pathak, H., Strate, P.G., Arora, K., Brinton, M.A., and Kumar, M. (2021). Neuroinvasion and encephalitis following intranasal inoculation of sars-cov-2 in k18-hace2 mice. Viruses *13*, 132. https://doi.org/10.3390/v13010132.

Kusnadi, A., Ramírez-Suástegui, C., Fajardo, V., Chee, S.J., Meckiff, B.J., Simon, H., Pelosi, E., Seumois, G., Ay, F., Vijayanand, P., and Ottensmeier, C.H. (2021). Severely ill COVID-19 patients display impaired exhaustion features in SARS-CoV-2-reactive CD8+ T cells. Sci. Immunol. *6*, 4782. https://doi.org/10.1126/SCIIMMUNOL.ABE4782/SUPPL_FILE.

Lai, C., Wang, K., Zhao, Z., Zhang, L., Gu, H., Yang, P., and Wang, X. (2017). C-C motif chemokine ligand 2 (CCL2) mediates acute lung injury induced by lethal influenza H7N9 virus. Front. Microbiol. *8*, 587. https://doi.org/10.3389/fmicb.2017.00587.

Landstra, C.P., and de Koning, E.J.P. (2021). COVID-19 and diabetes: understanding the interrelationship and risks for a severe course. Front. Endocrinol. *12*, 599. https://doi.org/10.3389/FENDO.2021.649525/BIBTEX.

Lee, A.J., and Ashkar, A.A. (2018). The dual nature of type I and type II interferons. Front. Immunol. *9*, 2061. https://doi.org/10.3389/FIMMU.2018.02061/BIBTEX.

Lee, K.S., Wong TY, Russ, B.P., Horspool, A.M., Miller, O.A., Rader, N.A., Givi, J.P., Winters, M.T., Wong, Z., Cyphert, H.A., et al. (2022). SARS-CoV-2 Delta variant induces enhanced pathology and inflammatory responses in K18-hACE2 mice. Preprint at bioRxiv. https://doi.org/10.1101/2022.01.18.476863.

Liao, Y., Wang, J., Jaehnig, E.J., Shi, Z., and Zhang, B. (2019). WebGestalt 2019: gene set analysis toolkit with revamped UIs and APIs. Nucleic Acids Res. *47*, W199–W205. https://doi.org/10.1093/nar/gkz401.

Martins, V.D., Silva, F.C., Caixeta, F., Carneiro, M.B., Goes, G.R., Torres, L., Barbosa, S.C., Vaz, L., Paiva, N.C., Carneiro, C.M., et al. (2020). Obesity impairs resistance to Leishmania major infection in C57BL/6 mice. PLoS Negl. Trop. Dis. *14*, e0006596. https://doi.org/10.1371/JOURNAL.PNTD.0006596.

Mazzoni, A., Salvati, L., Maggi, L., Capone, M., Vanni, A., Spinicci, M., Mencarini, J., Caporale, R., Peruzzi, B., Antonelli, A., et al. (2020). Impaired immune cell cytotoxicity in severe COVID-19 is IL-6 dependent. J. Clin. Invest. *130*, 4694–4703. https://doi.org/10.1172/JCI138554.

Melvin, W.J., Audu, C.O., Davis, F.M., Sharma, S.B., Joshi, A., DenDekker, A., Wolf, S., Barrett, E., Mangum, K., Zhou, X., et al. (2021). Coronavirus induces diabetic macrophage-mediated inflammation via SETDB2. Proc. Natl. Acad. Sci. USA *118*, e2101071118. https://doi.org/10.1073/PNAS.2101071118/SUPPL_FILE/PNAS.2101071118.SAPP.PDF.

Miller, L.R., Marks, C., Becker, J.B., Hurn, P.D., Chen, W.J., Woodruff, T., McCarthy, M.M., Sohrabji, F., Schiebinger, L., Wetherington, C.L., et al. (2017). Considering sex as a biological variable in preclinicalresearch. Faseb. J. *31*, 29–34. https://doi.org/10.1096/FJ.201600781R.

Mok, B.W.Y., Liu, H., Deng, S., Liu, J., Zhang, A.J., Lau, S.Y., Liu, S., Tam, R.C.Y., Cremin, C.J., Ng, T.T.L., et al. (2021). Low dose inocula of SARS-CoV-2 Alpha variant transmits more efficiently than earlier variants in hamsters. Commun. Biol. *4*, 1102. https://doi.org/10.1038/s42003-021-02640-x.

Moreau, G.B., Burgess, S.L., Sturek, J.M., Donlan, A.N., Petri, W.A., and Mann, B.J. (2020). Evaluation of K18- hACE2 mice as a model of SARS-CoV-2 infection. Am. J. Trop. Med. Hyg. *103*, 1215–1219. https://doi.org/10.4269/AJTMH.20-0762.

Morpheus, n d. https://software.broadinstitute.org/morpheus/.

Muniyappa, R., and Gubbi, S. (2020). COVID-19 pandemic, coronaviruses, and diabetes mellitus. Am. J. Physiol. Endocrinol. Metab. *318*, E736–E741.

Muñoz-Fontela, C., Dowling, W.E., Funnell, S.G., Gsell, P.S., Riveros-Balta, A.X., Albrecht, R.A., Andersen, H., Baric, R.S., Carroll, M.W., Cavaleri, M., et al. (2020). Animal models for COVID-19. Nature *586*, 7830. https://doi.org/10.1038/s41586-020-2787-6.

Neidleman, J., Luo, X., George, A.F., McGregor, M., Yang, J., Yun, C., Murray, V., Gill, G., Greene, W.C., Vasquez, J., et al. (2021). Distinctive features of SARS-CoV-2-specific T cells predict recovery from severe COVID-19. Cell Rep. *36*, 109414. https://doi.org/10.1016/J.CELREP.2021.109414.

Ng, W.H., Tipih, T., Makoah, N.A., Vermeulen, J.G., Goedhals, D., Sempa, J.B., Burt, F.J., Taylor, A., and Mahalingam, S. (2021). Comorbidities in SARS-CoV-2 patients: a systematic review and meta-analysis. mBio *12*, e03647-20. https://doi.org/10.1128/mBio.03647-20.

Nguyen, N.T., Chinn, J., De Ferrante, M., Kirby, K.A., Hohmann, S.F., and Amin, A. (2021). Male gender is a predictor of higher mortality in hospitalized adults with COVID-19. PLoS One *16*, e0254066. https://doi.org/10.1371/JOURNAL.PONE.0254066.

Nowakowska, M., Zghebi, S.S., Ashcroft, D.M., Buchan, I., Chew-Graham, C., Holt, T., Mallen, C., Van Marwijk, H., Peek, N., Perera-Salazar, R., et al. (2019). The comorbidity burden of type 2 diabetes mellitus: patterns, clusters and predictions from a large English primary care cohort. BMC Med. *17*, 145–210. https://doi.org/10.1186/s12916-019-1373-y.

O'Donnell, K.L., Pinski, A.N., Clancy, C.S., Gourdine, T., Shifflett, K., Fletcher, P., Messaoudi, I., and Marzi, A. (2021). Pathogenic and transcriptomic differences of emerging SARS-CoV-2 variants in the Syrian golden hamster model. Preprint at bioRxiv. https://doi.org/10.1101/2021.07.11.451964.

Oladunni, F.S., Park, J.G., Pino, P.A., Gonzalez, O., Akhter, A., Allué-Guardia, A., Olmo-Fontánez, A., Gautam, S., Garcia-Vilanova, A., Ye, C., et al. (2020). Lethality of SARS-CoV-2 infection in K18 human angiotensin-converting enzyme 2 transgenic mice. Nat. Commun. *11*, 6122. https://doi.org/10.1038/s41467-020-19891-7.

Olivers, J.C.. Venny. An interactive tool for comparing lists with Venn's diagrams. n.d. http://bioinfogp.cnb.csic.es/tools/venny/index.html.

Ouchi, N., Parker, J.L., Lugus, J.J., and Walsh, K. (2011). Adipokines in inflammation and metabolic disease. Nat. Rev. Immunol. *11*, 85–97. https://doi.org/10.1038/nri2921.

Pal, R., Bhadada, S.K., and Misra, A. (2021). COVID-19 vaccination in patients with diabetes mellitus: current concepts, uncertainties and challenges. Diabetes Metab. Syndr. *15*, 505–508. https://doi.org/10.1016/j.dsx.2021.02.026.

Paragh, G., Seres, I., Harangi, M., and Fülöp, P. (2014). Dynamic interplay between metabolic syndrome and immunity. Adv. Exp. Med. Biol. *824*, 171–190. https://doi.org/10.1007/978-3-319-07320-0_13.

Park, Y.M., Myers, M., and Vieira-Potter, V.J. (2014). Adipose tissue inflammation and metabolic dysfunction: role of exercise. Mo. Med. *111*, 65–72.

Patone, M., Thomas, K., Hatch, R., Tan, P.S., Coupland, C., Liao, W., Mouncey, P., Harrison, D., Rowan, K., Horby, P., et al. (2021). Mortality and critical care unit admission associated with the SARS-CoV-2 lineage B.1.1.7 in England: an observational cohort study. Lancet Infect. Dis. *21*,

1518–1528. https://doi.org/10.1016/S1473-3099(21)00318-2.

Peng, Y., Mentzer, A.J., Liu, G., Yao, X., Yin, Z., Dong, D., Dejnirattisai, W., Rostorn, T., Supasa, P., Liu, C., et al. (2020). Broad and strong memory CD4+ and CD8+ T cells induced by SARS-CoV-2 in UK convalescent individuals following COVID-19. Nat. Immunol. *21*, 1336–1345. https://doi.org/10.1038/s41590-020-0782-6.

Pettersson, U.S., Waldén, T.B., Carlsson, P.O., Jansson, L., and Phillipson, M. (2012). Female mice are protected against high-fat diet induced metabolic syndrome and increase the regulatory T cell population in adipose tissue. PLoS One *7*, e46057. https://doi.org/10.1371/JOURNAL.PONE.0046057.

Port, J.R., Adney, D.R., Schwarz, B., Schulz, J.E., Sturdevant, D.E., Smith, B.J., Avanzato, V.A., Holbrook, M.G., Purushotham, J.N., Stromberg, K.A., et al. (2021). Western diet increases COVID-19 disease severity in the Syrian hamster. Preprint at bioRxiv. https://doi.org/10.1101/2021.06.17.448814.

Rathnasinghe, R., Strohmeier, S., Amanat, F., Gillespie, V.L., Krammer, F., García-Sastre, A., Coughlan, L., Schotsaert, M., and Uccellini, M.B. (2020). Comparison of transgenic and adenovirus hACE2 mouse models for SARS-CoV-2 infection. Emerg. Microbes Infect. *9*, 2433–2445. https://doi.org/10.1080/22221751.2020.1838955.

Radvak, P., Kwon, H.J., Kosikova, M., Ortega-Rodriguez, U., Xiang, R., Phue, J.N., Shen, R.F., Rozzelle, J., Kapoor, N., Rabara, T., et al. (2021). SARS-CoV-2 B.1.1.7 (alpha) and B.1.351 (beta) variants induce pathogenic patterns in K18-hACE2 transgenic mice distinct from early strains. Nat. Commun. *12*, 6559. https://doi.org/10.1038/s41467-021-26803-w.

Rathnasinghe, R., Jangra, S., Cupic, A., Martínez-Romero, C., Mulder, L.C., Kehrer, T., Yildiz, S., Choi, A., Mena, I., De Vrieze, J., et al. (2021). The N501Y mutation in SARS-CoV-2 spike leads to morbidity in obese and aged mice and is neutralized by convalescent and post-vaccination human sera contributed equally. Preprint at medRxiv. https://doi.org/10.1101/2021.01.19.21249592.

Rawshani, A., Rawshani, A., Franzén, S., Sattar, N., Eliasson, B., Svensson, A.M., Zethelius, B., Miftaraj, M., McGuire, D.K., Rosengren, A., and Gudbjörnsdottir, S. (2018). Risk factors, mortality, and cardiovascular outcomes in patients with type 2 diabetes. N. Engl. J. Med. *379*, 633–644.

Rawshani, A., Kjölhede, E.A., Rawshani, A., Sattar, N., Eeg-Olofsson, K., Adiels, M., Ludvigsson, J., Lindh, M., Gisslén, M., Hagberg, E., et al. (2021). Severe COVID-19 in people with type 1 and type 2 diabetes in Sweden: a nationwide retrospective cohort study. Lancet Reg. Health Europe *4*. https://doi.org/10.1016/J.LANEPE.2021.100105.

Rha, M.S., and Shin, E.C. (2021). Activation or exhaustion of CD8+ T cells in patients with COVID-19. Cell. Mol. Immunol. *18*, 2325–2333. https://doi.org/10.1038/s41423-021-00750-4.

Roberts, J., Pritchard, A.L., Treweeke, A.T., Rossi, A.G., Brace, N., Cahill, P., MacRury, S.M., Wei, J., and Megson, I.L. (2021). Why is COVID-19 more severe in patients with diabetes? The role of angiotensin-converting enzyme 2, endothelial dysfunction and the immunoinflammatory system. Front. Cardiovasc. Med. *7*, 629933. https://doi.org/10.3389/FCVM.2020.629933.

Ronin, E., Lubrano di Ricco, M., Vallion, R., Divoux, J., Kwon, H.K., Grégoire, S., Collares, D., Rouers, A., Baud, V., Benoist, C., and Salomon, B.L. (2019). The nf-κb rela transcription factor is critical for regulatory t cell activation and stability. Front. Immunol. *10*, 2487. https://doi.org/10.3389/FIMMU.2019.02487/FULL.

Rosenke, K., Feldmann, F., Okumura, A., Hansen, F., Tang-Huau, T.L., Meade-White, K., Kaza, B., Callison, J., Lewis, M.C., Smith, B.J., et al. (2021). UK B.1.1.7 (Alpha) variant exhibits increased respiratory replication and shedding in nonhuman primates. Emerg. Microbes Infect. *10*, 2173–2182. https://doi.org/10.1080/22221751.2021.1997074.

Salvador, J.M., Mittelstadt, P.R., Guszczynski, T., Copeland, T.D., Yamaguchi, H., Appella, E., Fornace, A.J., Jr., and Ashwell, J.D. (2005). Alternative p38 activation pathway mediated by T cell receptor-proximal tyrosine kinases. Nat. Immunol. *6*, 390–395. https://doi.org/10.1038/ni1177.

Sanyaolu, A., Okorie, C., Marinkovic, A., Patidar, R., Younis, K., Desai, P., Hosein, Z., Padda, I., Mangat, J., and Altaf, M. (2020). Comorbidity and its impact on patients with COVID-19. SN Compr. Clin. Med. *2*, 1069–1076. https://doi.org/10.1007/S42399-020-00363-4.

Sarver, D.C., and Wong, G.W. (2021). Obesity alters Ace2 and Tmprss2 expression in lung, trachea, and esophagus in a sex-dependent manner: implications for COVID-19. Biochem. Biophys. Res. Commun. *538*, 92–96. https://doi.org/10.1016/J.BBRC.2020.10.066.

Seehusen, F., Clark, J.J., Sharma, P., Bentley, E.G., Kirby, A., Subramaniam, K., Wunderlin-Giuliani, S., Hughes, G.L., Patterson, E.I., Michael, B.D., et al. (2022). Neuroinvasion and neurotropism by SARS-CoV-2 variants in the K18-hACE2 mouse. Viruses *14*, 1020. https://www.mdpi.com/1999-4915/14/5/1020/htm.

Smith, A.G., Sheridan, P.A., Harp, J.B., and Beck, M.A. (2007). Diet-induced obese mice have increased mortality and altered immune responses when infected with influenza virus. J. Nutr. *137*, 1236–1243. https://academic.oup.com/jn/article/137/5/1236/4664595.

Sun, S.H., Chen, Q., Gu, H.J., Yang, G., Wang, Y.X., Huang, X.Y., Liu, S.S., Zhang, N.N., Li, X.F., Xiong, R., et al. (2020). A mouse model of SARS-CoV-2 infection and pathogenesis. Cell Host Microbe *28*, 124–133.e4. https://doi.org/10.1016/J.CHOM.2020.05.020.

Sun, Z., Yao, Y., You, M., Liu, J., Guo, W., Qi, Z., Wang, Z., Wang, F., Yuan, W., and Yu, S. (2021). The kinase pdk1 is critical for promoting t follicular helper cell differentiation. Elife *10*, e61406. https://doi.org/10.7554/eLife.61406.

Takahashi, T., Ellingson, M.K., Wong, P., Israelow, B., Lucas, C., Klein, J., Silva, J., Mao, T., Oh, J.E., Tokuyama, M., et al. (2020). Sex differences in immune responses that underlie COVID-19 disease outcomes. Nature *588*, 315–320. https://doi.org/10.1038/S41586-020-2700-3.

Tan, L., Wang, Q., Zhang, D., Ding, J., Huang, Q., Tang, Y.Q., Wang, Q., and Miao, H. (2020). Lymphopenia predicts disease severity of COVID-19: a descriptive and predictive study. Signal Transduct. Target. Ther. *5*, 33. https://doi.org/10.1038/s41392-020-0148-4.

Trayhurn, P. (2013). Hypoxia and adipose tissue function and dysfunction in obesity. Physiol. Rev. *93*, 1–21. https://doi.org/10.1152/PHYSREV.00017.2012.

Unnikrishnan, R., and Misra, A. (2021). Diabetes and COVID19: a bidirectional relationship. Eur. J. Clin. Nutr. *75*, 1332–1336. https://doi.org/10.1038/S41430-021-00961-Y.

Della Vedova, M.C., Muñoz, M.D., Santillan, L.D., Plateo-Pignatari, M.G., Germanó, M.J., Rinaldi Tosi, M.E., Garcia, S., Gomez, N.N., Fornes, M.W., Gomez Mejiba, S.E., and Ramirez, D.C. (2016). A mouse model of diet-induced obesity resembling most features of human metabolic syndrome. Nutr. Metab. Insights *9*, 93–102. https://doi.org/10.4137/NMI.S32907.

Viveiros, A., Rasmuson, J., Vu, J., Mulvagh, S.L., Yip, C.Y., Norris, C.M., and Oudit, G.Y. (2021). Sex differences in COVID-19: candidate pathways, genetics of ACE2, and sex hormones. Am. J. Physiol. Heart Circ. Physiol. *320*, H296–H304.

Westermann, A.J., and Vogel, J. (2018). Host-pathogen transcriptomics by dual RNA-seq. Methods Mol. Biol. *1737*, 59–75. https://doi.org/10.1007/978-1-4939-7634-8_4.

Winkler, E.S., Bailey, A.L., Kafai, N.M., Nair, S., McCune, B.T., Yu, J., Fox, J.M., Chen, R.E., Earnest, J.T., Keeler, S.P., et al. (2020). SARS-CoV-2 infection of human ACE2-transgenic mice causes severe lung inflammation and impaired function. Nat. Immunol. *21*, 1327–1335. https://doi.org/10.1038/s41590-020-0778-2.

Wong, T.Y., Hall, J.M., Nowak, E.S., Boehm, D.T., Gonyar, L.A., Hewlett, E.L., Eby, J.C., Barbier, M., and Damron, F.H. (2019). Analysis of the in vivo transcriptome of bordetella pertussis during infection of mice. mSphere *4*, e00154-19. https://doi.org/10.1128/MSPHEREDIRECT.00154-19.

Wong, T.Y., Horspool, A.M., Russ, B.P., Ye, C., Lee, K.S., Winters, M.T., Bevere, J.R., Miller, O.A., Rader, N.A., Cooper, M., et al. (2022a). Evaluating antibody-mediated protection against alpha, beta, and Delta SARS-CoV-2 variants of concern in K18-human ACE2 transgenic mice. J. Virol. *96*, e0218421.

Wong, T.Y.T., Lee, K.S., Russ, B.P., Horspool, A.M., Kang, J., Winters, M.T., Allison Wolf, M., Rader, N.A., Miller, O.A., Shiflett, M., et al. (2022b). Intranasal administration of BReC-CoV-2 COVID-19 vaccine protects K18-hACE2 mice against lethal SARS-CoV-2 challenge. npj Vaccines. https://doi.org/10.1038/s41541-022-00451-7.

Xiang, Q., Feng, Z., Diao, B., Tu, C., Qiao, Q., Yang, H., Zhang, Y., Wang, G., Wang, H., Wang, C., et al. (2021). SARS-CoV-2 induces lymphocytopenia by promoting inflammation and decimates secondary lymphoid organs. Front. Immunol. *12*, 1292. https://doi.org/10.3389/FIMMU.2021.661052/BIBTEX.

Yang, X.H., Deng, W., Tong, Z., Liu, Y.X., Zhang, L.F., Zhu, H., Gao, H., Huang, L., Liu, Y.L., Ma, C.M., et al. (2007). Mice transgenic for human angiotensin-converting enzyme 2 provide a model for SARS coronavirus infection. Comp. Med. *57*, 450–459.

Yinda, C.K., Port, J.R., Bushmaker, T., Offei Owusu, I., Purushotham, J.N., Avanzato, V.A., Fischer, R.J., Schulz, J.E., Holbrook, M.G., Hebner, M.J., et al. (2021). K18-hACE2 mice develop respiratory disease resembling severe COVID-19. PLoS Pathog. *17*, e1009195. https://doi.org/10.1371/journal.ppat.1009195.

Zhang, Y.-N., Zhang, Z.R., Zhang, H.Q., Li, X.D., Li, J.Q., Zhang, Q.Y., Liu, J., Li, Q., Deng, C.L., Shi, Z.L., et al. (2021). Cell Discovery Increased morbidity of obese mice infected with mouse-adapted SARS-CoV-2. Cell Discov. *7*, 74. https://doi.org/10.1038/s41421-021-00305-x.

Zhu, L., She, Z.G., Cheng, X., Qin, J.J., Zhang, X.J., Cai, J., Lei, F., Wang, H., Xie, J., Wang, W., et al. (2020). Association of blood glucose control and outcomes in patients with COVID-19 and pre-existing type 2 diabetes. Cell Metab. *31*. https://doi.org/10.1016/j.cmet.2020.04.021.

STAR★METHODS

KEY RESOURCES TABLE

REAGENT or RESOURCE	SOURCE	IDENTIFIER
Antibodies		
Goat anti-Mouse IgG (H + L) Secondary Antibody [HRP]	Novus Biologicals	Cat# NBP1-75130; RRID:AB_11012784
Goat anti-Mouse IgM Heavy Chain Secondary Antibody [HRP]	Novus Biologicals	Cat # NB7497; RRID:AB_524863
Bacterial and virus strains		
SARS-CoV-2 Alpha variant (hCoV19/England/204820464/2020)	BEI Resources	NR-54000
Chemicals, peptides, and recombinant proteins		
TRIReagent	Zymo Research	R2050-1
Triton X-100	Sigma-Aldrich	CAS Number: 9036-19-5
Ketamine	Patterson Veterinary	07-803-6637
Xylazine	Patterson Veterinary	07-808-1947
Euthasol (pentobarbital)	Patterson Veterinary	07-805-9296
SARS-CoV-2 nucleocapsid	Sino Biological	40588-V08B
SARS-CoV-2 RBD	Horspool et al., 2021	N/A
TMB reagent	Biolegend	421101
Tween 20	Sigma-Aldrich	P1379-1L
Dextrose (D-Glucose) Anhydrous	Fisher chemical	D16-500
Critical commercial assays		
Qubit Broad Range Assay Kit	Invitrogen	Q10210
R&D 9-plex mouse magnetic Luminex assay	Biotechne R&D systems	LXSAMSM
Qubit RNA High Sensitivity Assay kit	Invitrogen	Q32852
Deposited data		
Gene Expression Browser	Mendeley Data	
Raw RNAsequencing reads	NCBI SRA	
Experimental models: Organisms/strains		
Mouse: B6.Cg-Tg(K18-ACE2)2Prlmn/J	The Jackson Laboratory	Strain #: 034860
Oligonucleotides		
Nucleocapsid primers (F: ATGCTGCAATCGTGCTACAA; R: GACTGCCGCCTCTGCTC)	Winkler et al., 2020	N/A
TaqMan probe (IDT:/56-FAM/TCAAGGAAC/ZEN/AAC ATTGCCAA/3IABkFQ/)	Winkler et al., 2020	N/A
Software and algorithms		
Prism	GraphPadSoftware	Version 9
Venny 2.1	Oliveros, 2007-2015	https://bioinfogp.cnb.csic.es/tools/venny/
BioVenn	Hulsen et al., 2008	https://www.biovenn.nl/venndiagram.tk/create.php
WEB-based Gene SeT AnaLysis Toolkit	Liao et al. 2019	http://www.webgestalt.org/
Morpheus	Broad institute	https://software.broadinstitute.org/morpheus/
Ingenuity Pathway Analysis	Qiagen IPA Software	N/A
Other		
Mouse Diet, High Fat Fat Calories (60%), Soft Pellets	Bio-Serv	F3282

RESOURCE AVAILABILITY

Lead contact

Requests for additional information surrounding the described experiments and methods or reagents should be directed to the Lead Contact, Holly Cyphert (damron40@marshall.edu).

Materials availability

- This study did not generate any new unique reagents.
- The RNAseq datasets (gene expression browsers) generated in this study have been deposited to and are available at: https://doi.org/10.17632/zds9bng2yc.1.

Data and code availability

RNA sequencing data have been deposited at NCBI SRA: PRJNA875205 and are publicly available as of the date of publication. Accession numbers are listed in the Key resources table.

Any additional information required to reanalyze the data reported in this article is available from the lead contact on request.

EXPERIMENTAL MODEL AND SUBJECT DETAILS

Animal ethics statement

SARS-CoV-2 research experiments in mice were conducted in compliance with West Virginia University IACUC protocol #2009036460. K18-hACE2 transgenic mice were obtained for use from The Jackson Laboratory (B_6.Cg-Tg(K18-ACE2)2Prlmn/J; JAX strain number #034860). West Virginia University's Biosafety Level 3 Laboratory and Animal Housing facility were used for the cultivation of SARS-CoV-2 stocks and mouse challenge studies under IBC protocol #20-09-03.

Biosafety statement

Additional work in BSL2 conditions were performed after mouse tissue samples containing SARS-CoV-2 were treated with either 1% Triton (Sigma-Aldrich T8787) by volume (serum and supernatants) or TRIzol reagent (Zymo R2050-1) at a 1:1 ratio or greater (homogenates) to inactivate virus.

High fat diet induced K18-hACE2 mouse model of obesity and type 2 diabetes

Six-week-old male and female K18-hACE2 mice were provided a 60% fat diet (Bio-serv) *ad libitum* for 8 weeks to induce obesity and metabolic dysfunction. Age- and sex-matched control mice were concurrently provided a standard chow diet. Mouse weights were monitored weekly. At week 6, intraperitoneal glucose tolerance testing (IPGTT) was performed to assess insulin sensitivity. Mice were fasted for 6 h then injected with a solution of glucose in PBS (2% w/v) intraperitoneally (2 mg/g bodyweight). At 0, 15, and 60 min, blood glucose was measured from tail snips using a hand-held glucometer.

SARS-CoV-2 challenge strain cultivation

The Alpha variant of SARS-CoV-2 was obtained first from BEI: hCoV19/England/204820464/2020 (Alpha; NR-54000)(GISAID: EPI_ISL_683466). Vero E6 cells were grown to 90% confluency in a T150 flask before culture media was replaced with 20mL of viral stock in infection media. After 72 h of incubation at 37°C and monitoring for cytopathic effects, virus-containing cell media was pipetted off and transferred to two 15mL conical tubes. Media was centrifuged at 450 × g for 5 min at 4°C to pellet any cellular debris. Supernatant was then aliquoted into 1mL O-ring cryovials and stored as stocks at −80°C until use. Viral titers were confirmed by plaque assay.

METHOD DETAILS

K18-hACE2 mouse challenge with SARS-CoV-2

High fat diet and control male and female 6-week-old K18-hACE2 mice were health checked by West Virginia University Office of Laboratory Animal Resources vet staff before they were moved to the ABSL3 facility for SARS-CoV-2 challenge experiments. On the day of challenge, mice were anesthetized using an intraperitoneal injection of ketamine (Patterson Veterinary 07-803-6637) + xylazine (Patterson Veterinary 07-808-1947) (80 mg/kg). A suspension of the SARS-CoV-2 Alpha variant (10^3 PFU) was then administered

intranasally to each mouse by pipetting 25μL of the stock into each nare of the anesthetized mice (50 μL total).

K18-hACE2 mouse disease scoring

Beginning on the day of challenge, the overall health of the mice was evaluated using in-person assessments of rectal temperature, weight, appearance, and behavior. In addition to in-person checks, mice were monitored using the SwifTAG Systems video monitoring system. Mice received daily scores for activity (0-3), appearance (0-2), changes in respiratory phenotype (0-2), eye closure/conjunctivitis (0-2) and weight loss (0-4). Each score was based on a scale where 0 indicated a normal mouse phenotype and the numerical scale represents increasingly severe phenotypes. The combined total of each category's scores were awarded to each mouse as its daily disease score. Mice that reached 20% weight loss experienced a significant drop in temperature and/or a disease score of 5 were euthanized in compliance with predetermined humane endpoints. Daily health checks were performed until day 11 post-challenge.

Mouse necropsy and tissue collection

On the day of euthanasia, mice were administered an intraperitoneal injection (390 mg/kg) of Euthasol (pentobarbital) (Patterson Veterinary 07-249 805-9296) diluted in 0.9% sterile NaCl. Once mice were unresponsive, blood was collected via cardiac puncture in serum separator tubes (BD, 365,967). To separate the serum, each tube was centrifuged for 5 min at 15,000 × g. Mice were dissected to collect the lung and brain tissues as well as nasal wash fluid for downstream analysis. Nasal wash fluid was collected by pushing 1mL sterile PBS by catheter through the nasal pharynx. Right lobes of the lung were homogenized in 1mL sterile PBS using gentleMACS C tubes (Miltenyi Biotec, 130-096-334) and the m_lung_02 program on the gentleMACS Dissociator (Miltenyi Biotec, 130-093-235). Whole brains were homogenized similarly. For RNA analysis 300μL of lung homogenate, or 500μL or brain homogenate was added to 1mL TRIzol Reagent (Zymo R2050-1). For nasal wash RNA analysis, 500μL of nasal wash was added to 500μL of TRIzol Reagent. For cytokine analysis, 300μL of lung homogenate was centrifuged at 15,0000 × g for 5 min and the supernatant was collected.

Quantification of SARS-CoV-2 nucleocapsid RNA

The Direct-zol RNA miniprep kit (Zymo, R2050) was used according to the manufacturer's protocol to purify RNA from the nasal wash, lung, and brain homogenates of SARS-CoV-2 challenged mice. Resulting RNA concentrations were quantified using the Qubit 3.0 Fluormeter and Qubit Broad Range Assay Kit (Invitrogen, Q10210). SARS-CoV-2 nucleocapsid RNA was quantified by qPCR using the Applied Biosystems TaqMan RNA-to-CT One-Step Kit (Thermo Fisher, 4,392,938). qPCR reactions for each sample and tissue were prepared in triplicate in Micro-Amp Fast optical 96 well reaction plates (Applied Biosystems, 4,306,737) and contained: 2XTaqMan RT-PCR Mix, 900nM Forward and reverse primers, 250nM TaqMan probe, 40X TaqMan RT enzyme mix and 100ng RNA template. RNA template from nasal wash samples was added at a set volume of 2 μL because of low RNA concentrations. Nucleocapsid primers (F: ATGCTG CAATCGTGCTACAA; R: GACTGCCGCCTCTGCTC); and TaqMan probe (IDT:/56-FAM/TCAAGGAAC/ ZEN/AACATTGCCAA/3IABkFQ/) synthesized according to Winkler et al. (2020) (Winkler et al., 2020). qPCR reactions were performed on the StepOnePlus Real-Time System machine using the following parameters: Reverse transcription for 15 min at 48°C, activation of AmpliTaq Gold DNA polymerase for 10 min at 95°C, and 50 cycles of denaturing for 15 s at 95°C and annealing at 60°C for 1 min.

Serological analysis

Anti-nucleocapsid and anti-RBD specific IgG as well as IgM antibodies were measured in the serum of SARS-CoV-2 challenged mice by ELISA. High binding 96-well plates (Pierce, 15,041) were coated overnight (4°C) with RBD or nucleocapsid at a concentration of 2 μg/μL. On the day of, plates were washed 3× with PBS-0.1% Tween 20, then incubated shaking for 1 h with 200μL of 3% non-fat milk in PBS-0.1% Tween 20 per well to block. After blocking, the plates were washed 4× with PBS-0.1% Tween 20 before adding sample. Mouse serum was diluted 1:20 in the wells of row A with 1% non-fat milk in PBS-0.1% Tween 20, then serially diluted 1:2 into 1% non-fat milk in PBS-0.1% Tween 20 across the concurrent wells of two plates (total of 15 dilutions). Plates were then incubated shaking for 1 h with sample before being washed again 4× with PBS-0.1% Tween 20. Secondary antibody diluted 1:2,000 for IgG (Goat anti-mouse IgG (H + L) HRP (Novus biological, NBP1-75130)) or 1:10,000 for IgM (Goat anti-mouse IgM HRP (Novus biological, NB7497)) in 1% non-fat milk in PBS-0.1% Tween 20 was then added to all wells at a volume of 100μL, and plates were

incubated shaking for an additional 1 h. After incubation, unbound secondary was washed away with 5× washes of PBS-0.1% Tween 20. TMB reagent (Biolegend, 421,101) was added to each well at a volume of 100μL to develop the reaction. After 15 min in the dark, the reaction was stopped using 50μL 2N Sulfuric acid. Assays were analyzed at 450nm using the Synergy H1 plate reader. Antibody titers were quantified using area under the curve analysis in GraphPad Prism v.9.0.0.

Cytokine analysis

To measure IFN-γ as well as other cytokines, samples of lung supernatant and serum from each mouse were run on the R&D 9-plex mouse magnetic Luminex assay (Ref LXSAMSM). The manufacturer's protocols were followed to prepare and run samples. The plate was analyzed on the Luminex Magpix to calculate concentrations (pg/mL) based on of the individual standard curves for each cytokine. MSD assay plates were analyzed using the Meso Scale Discovery Sector 2400.

Illumina library preparation

RNA concentrations from SARS-CoV-2 challenged mouse lung homogenates were measured with the Qubit 3.0 Fluormeter using the RNA High Sensitivity kit (Invitrogen, Q32852) and RNA integrity was assessed using an Agilent TapeStation. RNA was DNAased before library preparation. Illumina sequencing libraries were created with the KAPA RNA Hyper-Prep Kit with RiboErase (Basel, Switzerland). Resulting libraries passed standard Illumina quality control PCR and were sequenced on an Illumina NovaSeq s4 4000 at Admera Health (South Plainfield, NJ).

QUANTIFICATION AND STATISTICAL ANALYSIS

RNA sequencing and *in silico* bioinformatics analysis

A total of ~100 million 150 base pair reads were acquired per SARS-CoV-2 challenged mouse lung sample. Sequencing data will be deposited to the Sequence Read Archive. The reads were trimmed for quality and mapped to the *Mus musculus* reference genome using CLC Genomics Version 21.0.5. An exported gene expression browser table is provided as supplemental materials (Table S1). Statistical analysis was performed with the Differential Expression for RNA Seq tool and genes were annotated with the reference mouse gene ontology terms. PCA plots were formed in CLC Genomics Version 21.0.5. Quantification of the number of activated or repressed genes unique to each experimental group was performed using Venny 2.1 (Olivers, n.d.) and visually modeled using the WEB-based BioVenn (Hulsen et al., 2008). Genes from each experimental comparison with significant fold changes compared to no-challenge (Bonferroni $\leq$0.04) were submitted to the WEB-based Gene SeT AnaLysis Toolkit's OverRepresentation Analysis (ORA) software compared to the reference set "affy mg u74a" to determine GO terms from gene ontology and biological process databases (FDR $\leq$0.05) (Liao et al., 2019). GO Term heat maps were generated using Morpheus (Morpheus, n.d.). To analyze the expression of the hACE2 transgene, the RNA reads were mapped to the human ACE2 gene (GRCh38). SARS-CoV-2 reads were analyzed by mapping the reads to the SARS-CoV-2 WA-1 reference genome. hACE2 and viral reads were normalized by dividing counts per 50M total reads in each sample.

Ingenuity pathway analysis

RNAseq fold change gene expression data was submitted to Ingenuity Pathway analysis using a cut off value of p=0.05. Pathways that were statistically enriched were exported and plotted into heat maps using Morpheus as described above.

Statistical analysis

Statistical tests were performed in GraphPad Prism v.9.0.0. K18-hACE2 mouse studies were performed with an n = 5 per experimental group. In preluding experiments to determine the challenge dose, n $\geq$ 3. Kaplan Meier survival curves were analyzed using Mantel-Cox log rank tests. Student's t-tests were used for comparisons made between two groups. When three or four groups were being compared, statistical differences were assessed using one-way ANOVA with Dunnett's multiple comparisons test or two-way ANOVA with Tukey's multiple comparisons test for parametric data. For any non-parametric data, Kruskal-Wallis tests with Dunn's multiple comparisons tests were used.